Satellite Applications Report: Fog Detection and Monitoring

With support from
SPAWAR Systems Center Charleston (Code 66)

June 30, 2006

Matthew A. Lazzara
Antarctic Meteorological Research Center
Space Science and Engineering Center
University of Wisconsin-Madison
1225 West Dayton Street
Madison, Wisconsin, USA 53706
Voice: (608) 262-0436
FAX: (608) 263-6738
mattl@ssec.wisc.edu
http://amrc.ssec.wisc.edu
ftp://amrc.ssec.wisc.edu

UW SSEC Publication No.06.07.L1

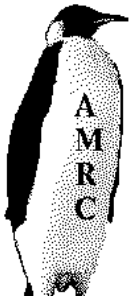

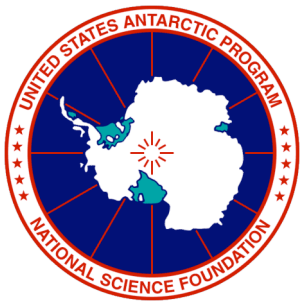

Compiled in 2006 by the
Antarctic Meteorological Research Center
Space Science and Engineering Center
University of Wisconsin-Madison

This report may be cited as:

Lazzara, M.A., 2006: Satellite Application Report: Fog Detection/Monitoring. UW SSEC Publication No.06.07.L1. Space Science and Engineering Center, University of Wisconsin-Madison, 44 pp. [Available from The Schwerdtfeger Library, University of Wisconsin-Madison, 1225 W. Dayton St., Madison, WI 53706.]

This report is available from:

The Schwerdtfeger Library
University of Wisconsin-Madison
1225 W. Dayton St., Madison, WI 53706
UW SSEC Publication No.06.06.L1
(http://library.ssec.wisc.edu/).

Or on-line at:

http://amrc.ssec.wisc.edu/Satellite-Applications-Report-Fog.pdf

This report is dedicated to all of the men and women of the United States Antarctic Program and other nations Antarctic programs who deal with serious impacts and effects of Antarctic fog.

Table of Contents

Introduction

Fog is one of the top three weather forecasting challenges faced by United States Antarctic Program (Cayette, pers. Comms. 2000). With McMurdo Station suffering from one to four days with fog each month on average (Lazzara, 2006), to as much as five times that number for the nearby skiways/airfields, the ability to detect and monitor fog, as well as forecast its evolution, is critical for safety, aviation and other logistics in the region (See Figure 1). Recently, web cameras have been installed in the McMurdo region with an aim of aiding the forecasting of fog (See Figure 2). Along with the aid of automatic weather station (AWS), METAR, and radiosonde observations, satellite observations will be an important tool used to detect and monitor fog events.

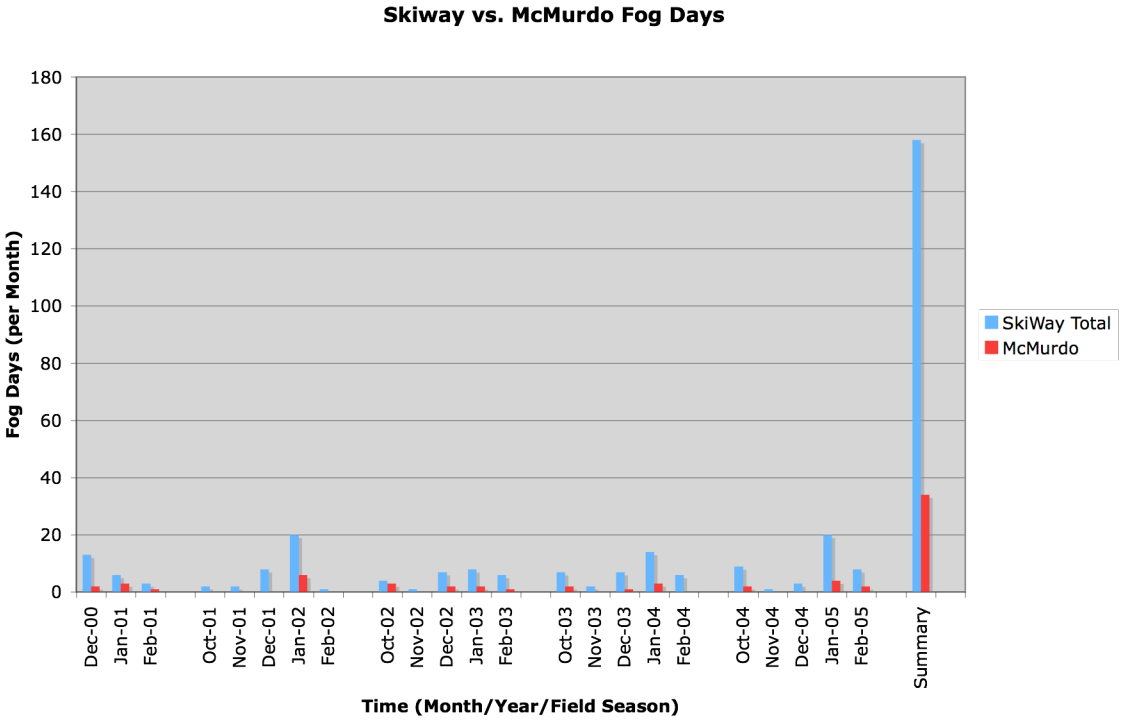

Figure 1 A graph showing McMurdo Station only experience 18 percent of the fog events in the McMurdo Sound Basin, when comparing with fog occurrences at the three nearby Skiways: Ice Runway, Williams Field and Pegasus Field for late 2000 through the 2005 field season. Please note the Skiway totals do not have any duplicate data. A fog day is a day in which at least one observation report includes fog.

a. b. c.

Figure 2. A web cam capture of a fog event from the Williams Field web camera from February 2, 2006. (*Courtesy of Art Cayette*)

Historical Use Of Satellites For Fog Monitoring: AVHRR

Single Channel Detection

One of the early applications of satellite observations was for observing fog. Early polar orbiting and from geostationary platforms used the visible channel (typically near 0.67-micron wavelength) for fog monitoring. These early observations were not often able to exploit the single infrared channel for this kind of information, due to the fact that fog often is observed to be at the same temperature as its surroundings. Hence, fogged in regions was unable to be detected clearly as compared to clear, fog free regions nearby. Later as other spectral channels became available, other single channels where applied, such as the 3.7-micron channel. This report will not review this era as little is documented on applications or uses in the Antarctic.

Two Channel Detection

In the mid-1980s the first bi-spectral (two channel) applications for fog were developed employing satellite data. Using the Advanced Very High Resolution Radiometer (AVHRR) on the National Oceanic and Atmospheric Administration (NOAA) satellite series, Eyre et al. (1984) exploited spectral differences in fog signatures in the 3.7 micron and 11 micron wavelengths (this is supported in work that was theoretically calculated by Hunt in 1973). This technique was targeted for detecting fog at night, when the visible sensors of the satellite were not available (Eyre et al. 1984). The method consisted of a simple amplified temperature difference. Prior to this study, the fog observations were only made using the visible sensor (0.67-micron wavelength). This method would receive its first test as documented in Turner et al. (1986), which was a critical application of Eyre's work over England.

Ellrod published his work on applying Eyre's bi-spectral method to the Geostationary Operational Environmental Satellite (GOES) (Ellrod, 1991, 1994 and 1995). Before the close of the decade this method would become operationally used in the United States National Weather Service. See Figure 3 for an example of this method applied to AVHRR data over the Antarctic.

Meantime, Wetzel et al. (1996) continued to study and learn about land based fog characteristics, including drop effective radius and optical depth, using AVHRR and employing balloons for validation. Lee, et al. (1997) critically reviewed bi-spectral methods with GOES-8 and -9 data. They concluded that bi-spectral and reflectance methods for fog detection are both important, and each should be used at a specific time of day for the best results (bi-spectral at night, and reflectance at day and sunset/sunrise times).

The landmark work by Eyre and applications by Ellrod faces serious challenges when applied in the Antarctic. These methods may highlight fog, but not in all cases. Since the critical use of these applications is at night, they may not work well during the austral summer, when there is likely both a peak fog occurrence (Lazzara, 2006), and nearly 24 hours of sunlight, degrading the technique. Also, the same method may highlight other features (such as clouds clearly seen in Figure 3), or miss fog features. These challenges, combined with the availability of advanced satellite imaging, give rise to the opportunity to improve fog detection methods from satellite platform.

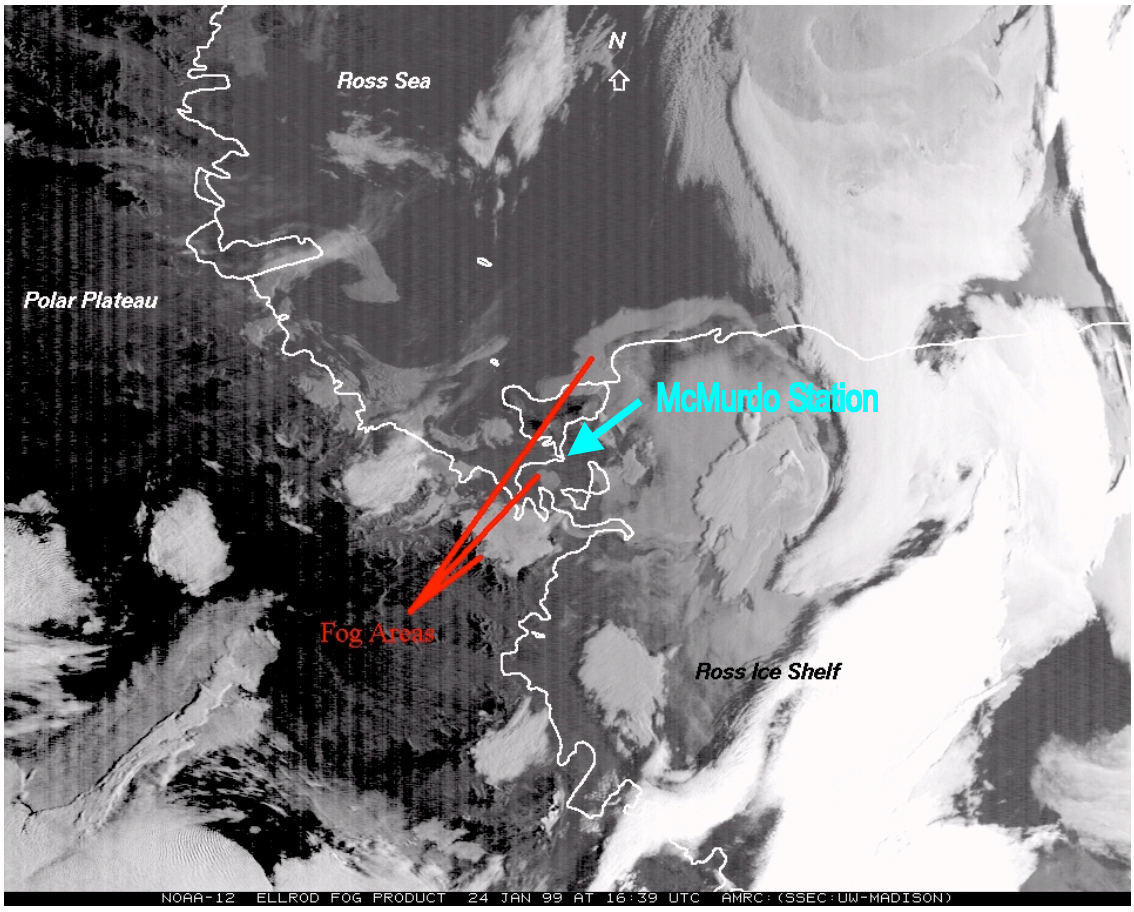

Figure 3. A sample AVHRR bi-spectral fog product image over Ross Island Antarctic just hours before a fog event strikes Williams Field, near McMurdo Station, Antarctica. This image follows methods outlined by Erye et al. (1984) and Ellrod (1994), with manual contrast stretch enhancement.

Applications Of An Advanced Satellite Sensor System: MODIS

Description

A full technical description of the Moderate-Resolution Imaging Spectroradiometer (MODIS) sensor is described in Appendix B of this report. This sensor system is on board the Terra and Aqua satellites – NASA's two lead spacecraft in the Mission To Planet Earth (MTPE) Earth Observing System (EOS). With a heritage from other satellite sensors such as AVHRR, Sea-viewing Wide-Field-of-view Sensor (SeaWiFS), Landsat Thematic Mapper and Nimbus 7 Coastal Zone Color Scanner (CZCS), MODIS brings significant improvements in the spectral and spatial resolution of these sensors.

Single Band Detection

As with AVHRR, the MODIS sensor can be used channel by channel to detect fog events. Figures 4 and 5 show examples in the visible (0.64 microns) and shortwave infrared (3.9-micron) range that are very much like those the AVHRR offers. Of course, the MODIS in the visible bands offers higher spatial resolution, up to 250 meters (See Figure 6), as compared to the 1.1 kilometer on AVHRR.

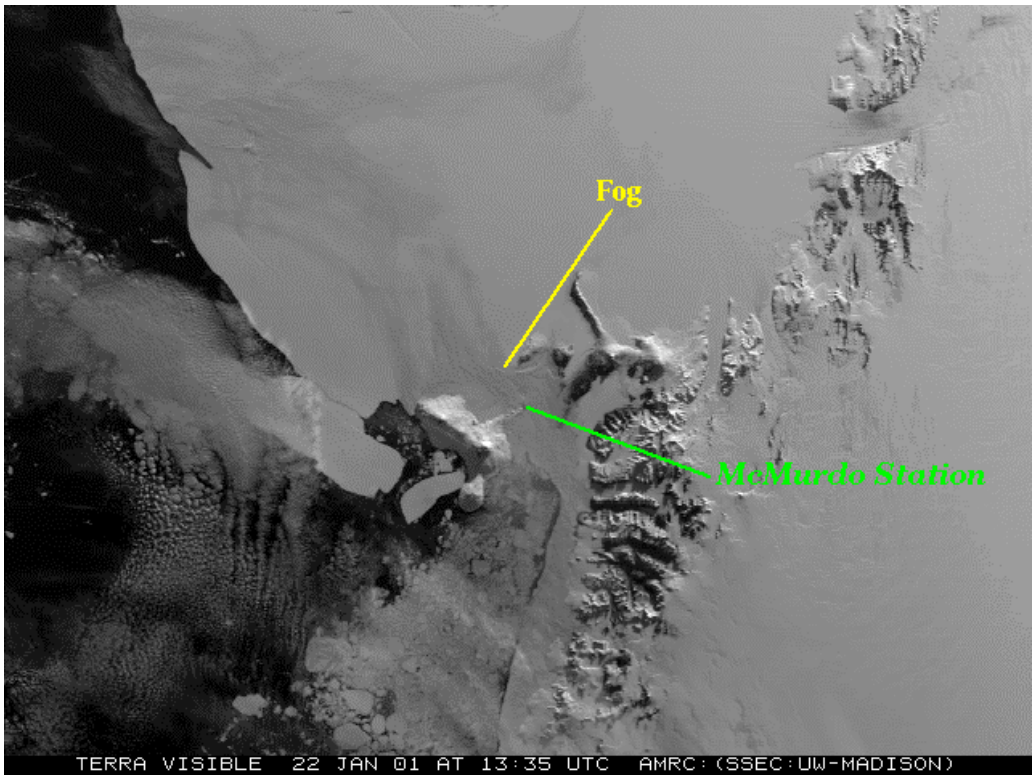

Figure 4. A fog event from January 22, 2001 as captured by the Terra satellite in the visible (0.64 micron) channel, constrast stretched to enhance the thin fog over the McMurdo Sound.

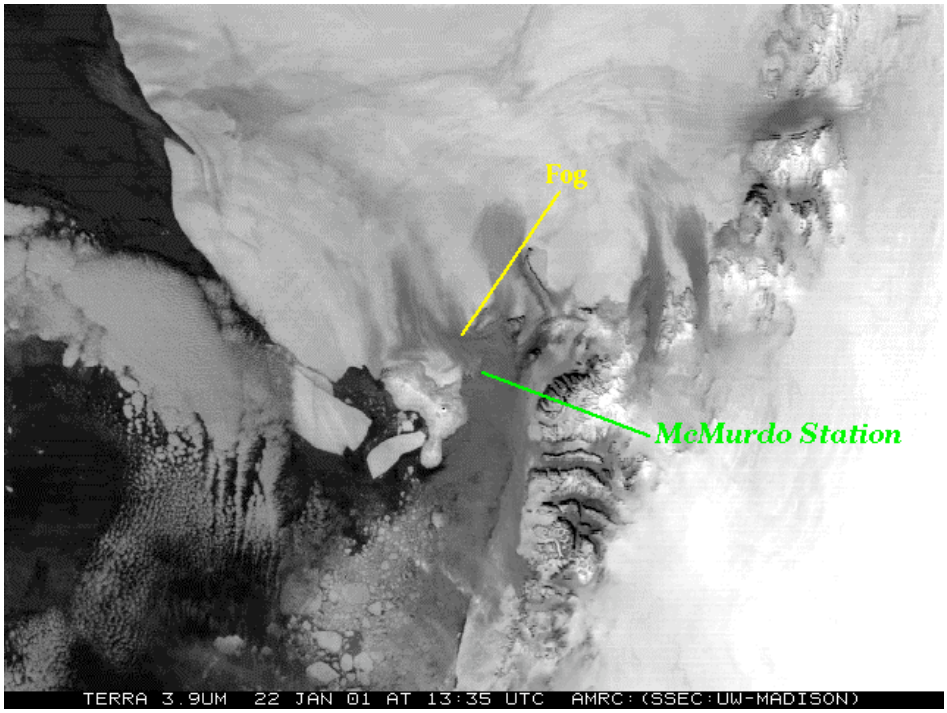

Figure 5. The same fog event as in figure 2, however seen with the shortwave infrared (3.97 micron) channel, and constrast stretched to enhance the fog over the region. Note the katabatic outflow from the Skelton and Mulock Glaciers is also enhanced.

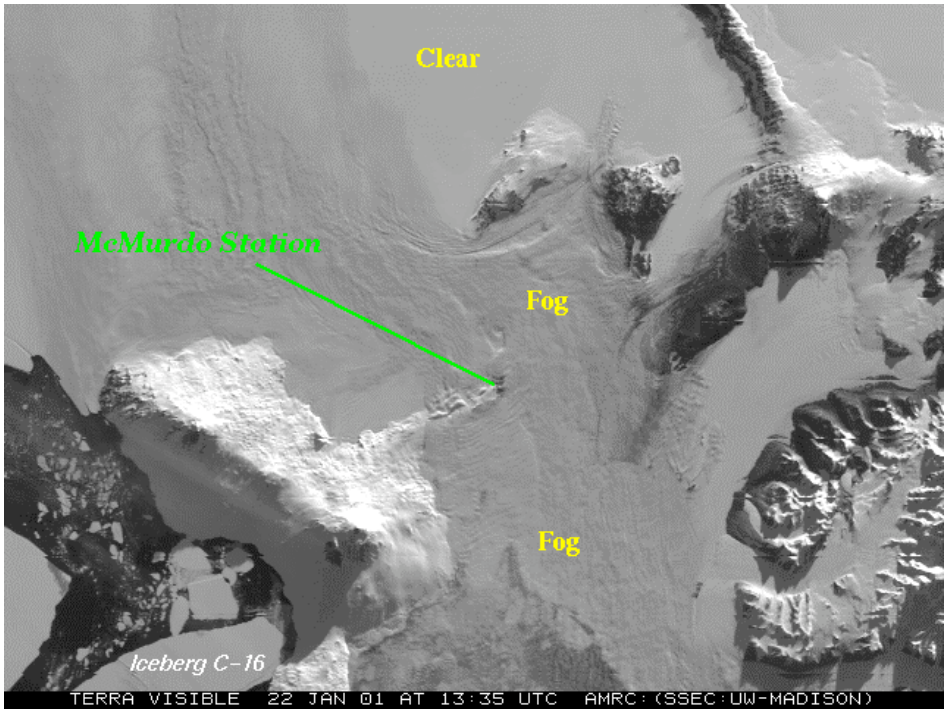

Figure 6. Same fog event as in figure 2, however, this is the visible image at 250 meters resolution.

Dual-Channel Detection

As with the AVHRR sensor, it is also possible to apply the Eyre and Ellrod dual channel methods for enhancing and detecting fog. As seen in Figure 7, the same approach can indeed be taken, however the nature of the method also enhance high thin cirrus as well. This method is intended for use at night, which diminishes its use during the peak season for fog during austral summer, which has 24 hours of sunlight. This, along with the challenges of applying this method near snow-covered regions can make visual interpretation challenging for the forecaster. This display was generated in the Man computer Interactive Data Access System (McIDAS) processing system.

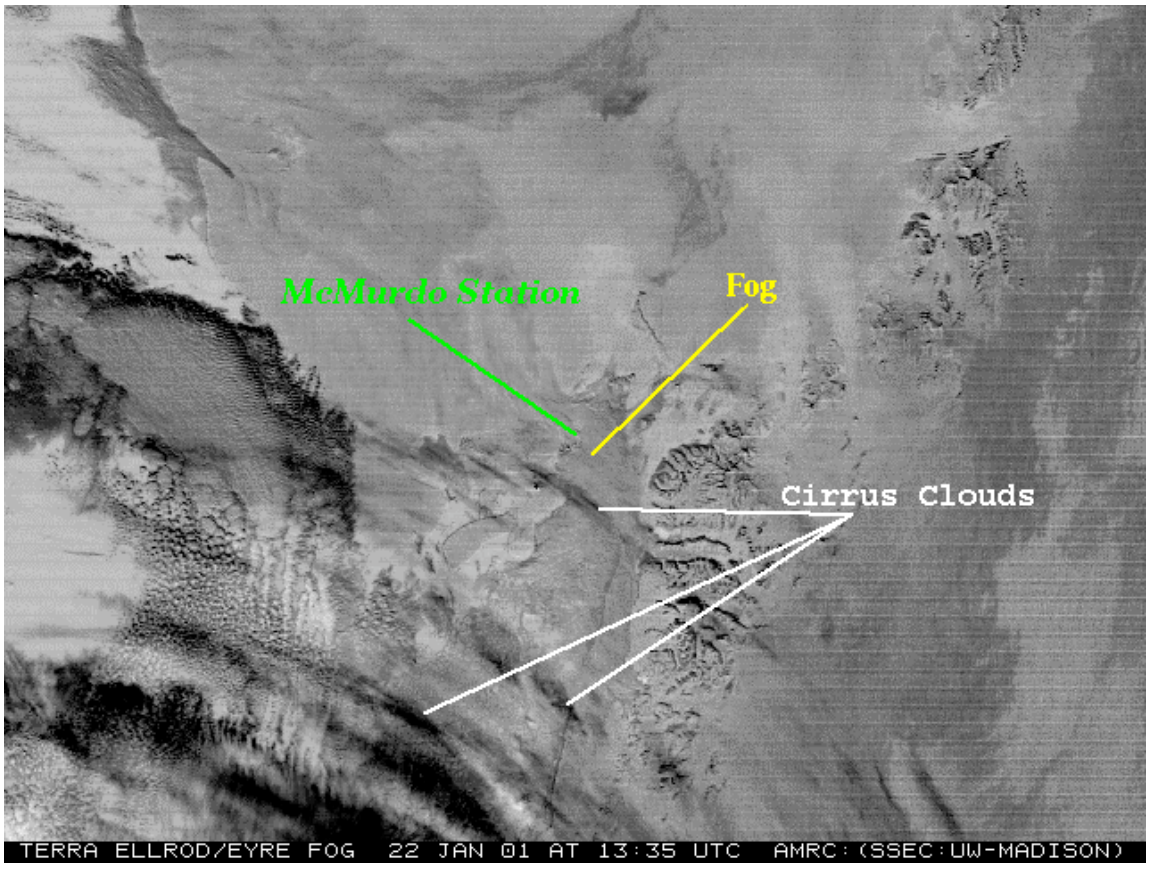

Figure 7. The Eyre/Ellrod dual channel method for enhancing/detecting fog for the same case as in figure 1, with constract stretch. Note the impact the cirrus clouds have on this enhancement.

Multi-Channel Detection

With the availability of additional spectral channels on the MODIS sensor, it is possible to consider other spectral channels applied toward the detection of fog. There are a few approaches that can be considered including spectral band color combinations, differential spectral band color combinations, and mathematical combinations. Following sections will cover more sophisticated methods including principal component images, and spectral test methods combined with cloud detection or masking.

Spectral Band Color Combinations

One method of combining multiple spectral channels is the use of a "three channel combination" via colorizing three selected channels individually through the colors of red, green and blue (RGB). The result of running the data values through these colors and then combining them may automatically enhance the features inherent in each of the single channels, combined into a 24-bit display.

One additional channel to use in this combination is the 1.6-micron channel (band 6 on the MODIS sensor), which offers the ability to provide discrimination assistance against the snow/ice background. Unfortunately, this channel is not available on the MODIS instrument onboard the Aqua satellite as that one channel failed before launch (Batson, pers. comms., 2001). Alternative channels that offer some of the same ability include the 1.24-micron channel (band 5), and 2.11-micron channel (band 7). Other channels that might seem helpful, turn out not to be. One such example is the 1.38-micron channel (band 26), where high thin cirrus clouds are enhanced over the fog below. Note that an automatic contrast stretch has been applied to the examples show in Figures 8 and 9. This automatic method will vary depending on the brightness in the imagery from the entire scene. Figure 10 shows the differences in a few of the same combinations, however in these cases, the automatic stretch is done via a binning histogram analysis rather than a linear analysis.

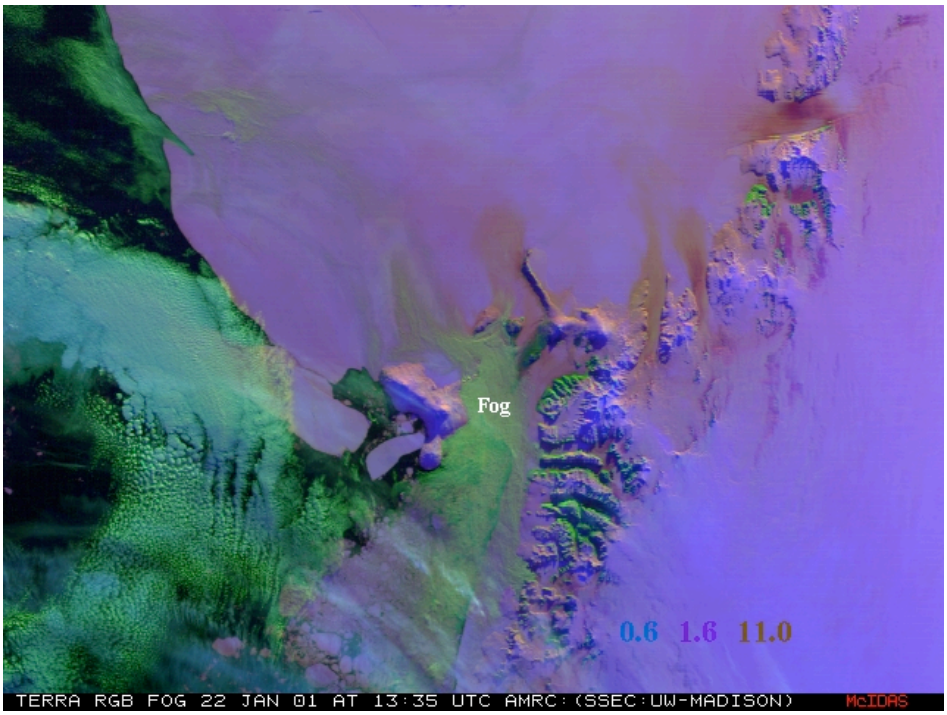

Figure 8. An RGB three channel color combination of the visible 0.6 micron, 1.6 micron and infrared 11.0 micron channels. Each channel is automatically contrast stretched before combining. The fog area can be seen in the green tinged cloud region labeled. Notice katabatic flow regions and other land features are also enhanced.

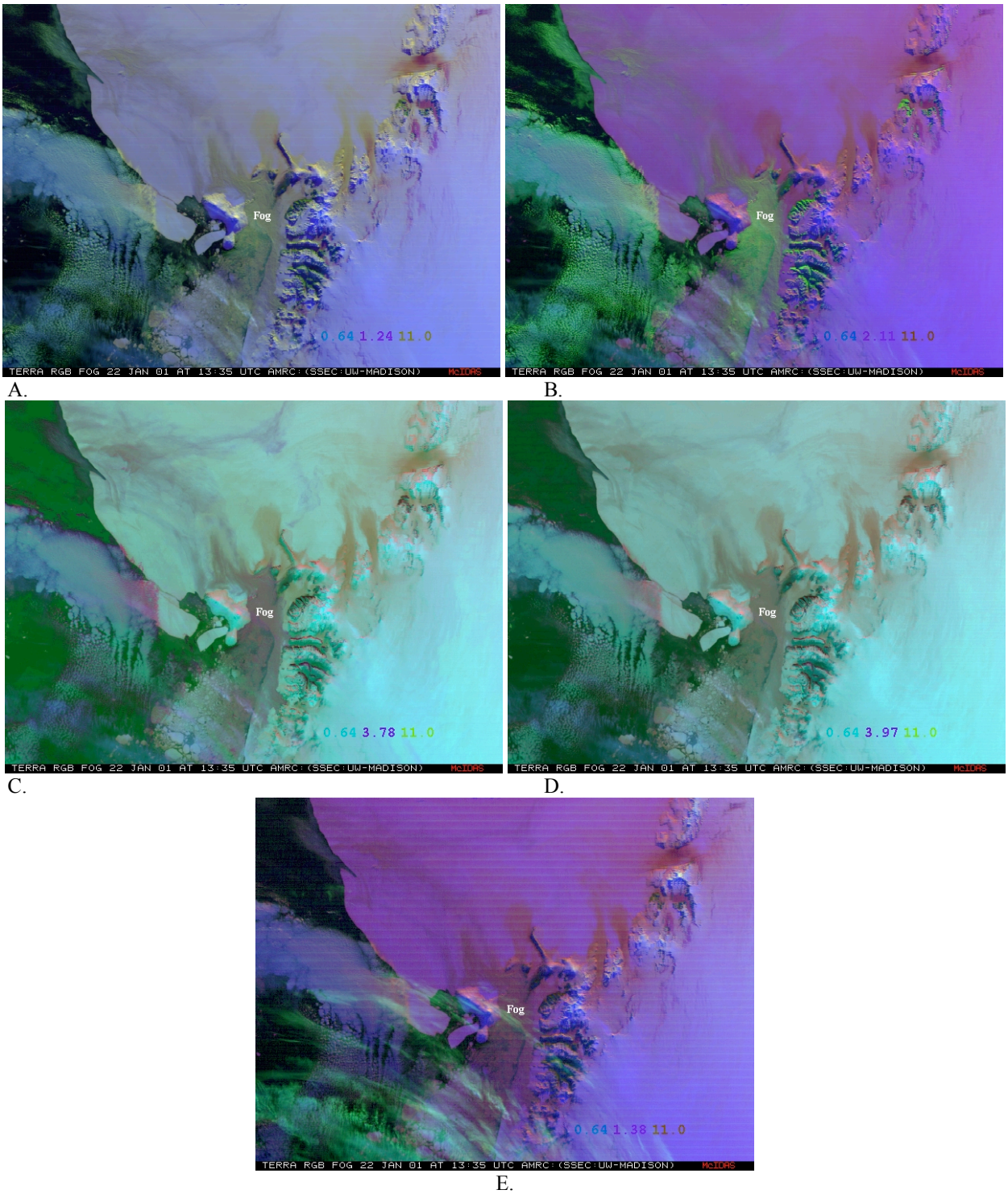

Figure 9. Samples of other RGB combined images. Some have possibilities for enhancing fog, others have problems with cirrus clouds impacting the enhancement (especially E.).

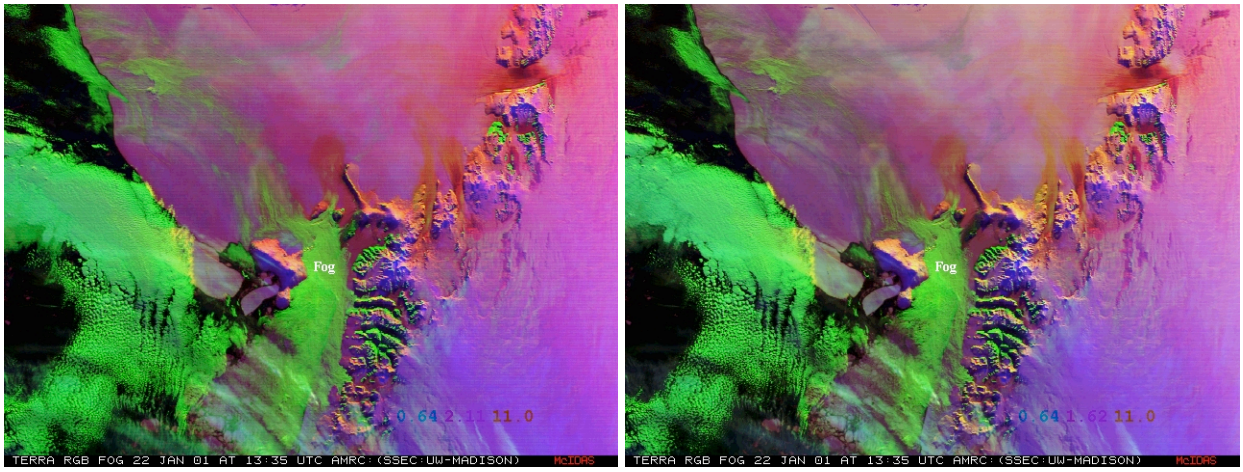

A. B.

Figure 10. Two examples of the same RGB as in figure 8 and 9, however the automatic contrast stretch uses a histogram styled analysis with 24 bins.

Differential Spectral Band Color Combinations

Beyond using the RGB method on single channels, it is also worth considering the same application applied toward mathematical combinations of channels such as via brightness, albedo or temperature differences between channels. As shown in the example in Figure 11, this is a RGB combination of the 1.6-micron minus the 11.0-micron for the red, the 3.9-micron minus the 11.0-micron for the green, and the 7.3-micron minus the 6.7-micron channel for the blue. A product demonstrated by EUMETAT for its new Meteosat Second Generation satellite and its sensor the SEVIRI was inspiration of the examples shown in the figure.

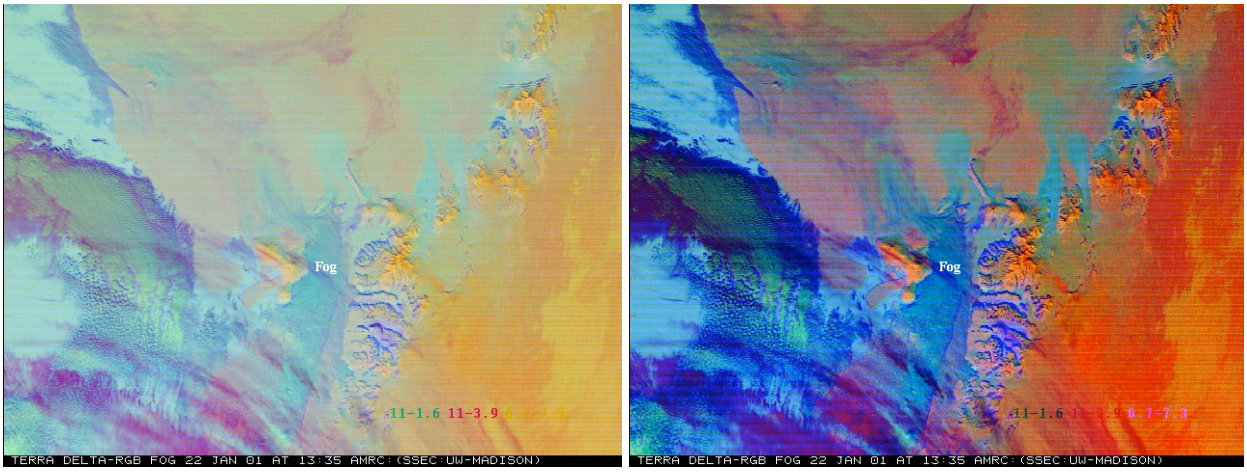

A. B.

Figure 11. Two examples of a "differential" spectral band color with automatic contrast stretch (A. standard B. histogram styled analysis with 24 bins.) See text for channel combinations used.

The examples shown in figure 11 utilize channels that are not typically used for the detection of fog. The blue contribution uses channels that are sensitive to water vapor, but also can favor upper level water vapor features, which may explain the enhancement of the thin cirrus in the lower left quadrant of the both images. Figure 12 below shows a selection of channels that may offer more information focused at the level fog events occur around the Ross Island region.

Mathematical Combinations

Direct use of the spectral channels can be done via mathematical combinations such as ratios of channels or even utilized via polynomial expressions. An initial review of a fog scene, as shown in figure 12, denotes a scatter diagram plot the difference between two channels (in this case the 2.11-micron minus the 0.645-micron spectral channels plotted against the 3.78-micron minus the 3.97-micron spectral channels). The conversion of this into a mathematical formulation is in progress at the University of Wisconsin. It is not clear if this method will be universally applicable to all fog cases; however, it may work for a class of fog types that affect the McMurdo Sound and Ross Island region.

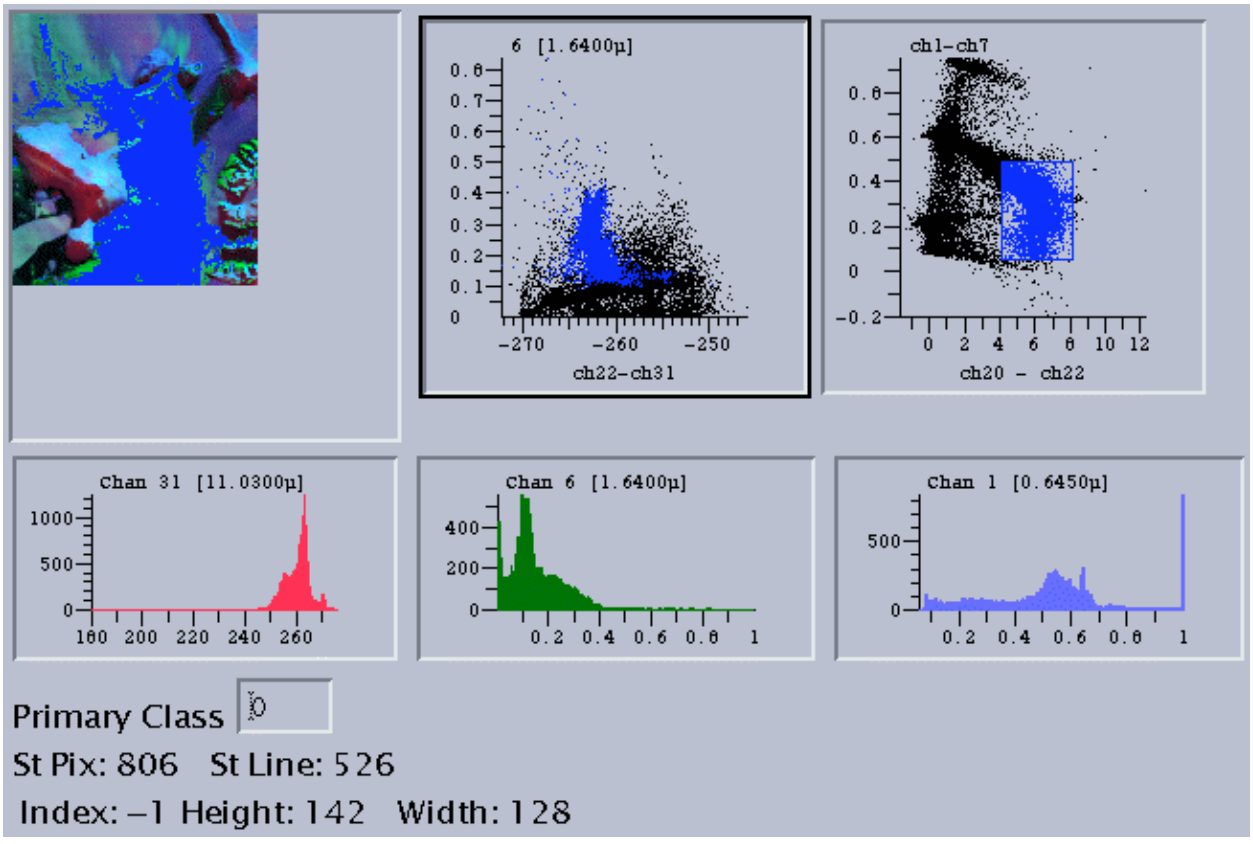

Figure 12. A scatter diagram analysis of a fog event in the McMurdo Sound. Blue colors in the satellite image and in the scatter diagrams are the pixels with fog. The scatter diagram on the right shows the fog separated from other features in the satellite field of view.

Principal Component Image Method

Utilization of software created by Don Hilger at the Cooperative Institute for Research in the Atmosphere (CIRA) at the Colorado State University provides another method for detecting fog. It is an application of Principal Component Analysis (PCA). The software takes in multiple spectral channels of the satellite observations, and outputs new principal component "images" where the first "image" depicts the features from the original observation that explain the most variance of the data. Similarly, the second "image" depicts the features from the observation that explain the second most variance of the data, etc. The PCA method is very much akin to the Empirical Orthogonal Functions (EOF) analysis method applied to multivariate data. EOF analysis provides information on variance both spatially and temporally, while PCA provides information on variance spatially.

Examples of this can be seen in figure 13. It is important to remember that these images are the result of the analysis and are not a specific channel or band of the MODIS data. In this case, the variance of the imagery among the input spectral channels has a variety of strong signals. Clearly seen in the first principal component in figure 13, the ice surface has a strong signal. However, the first and second principal components do show the fog region over the McMurdo Sound region. The third component focuses on the visible portions of the spectrum while the fourth is a mix of information from the channels – nearly matching some of the prior example enhancement methods.

With the fog clearly enhanced in the top components, figures 14 and 15 show red-green-blue combinations of top principal component images. Figure 14 shows a combination of the first three components combined via a red-green-blue combination (as described above). However, as shown in figure 15, the combination of just the first two principal components, with twice the weighting (via both red and green) on the second component image, shows most of the fog signal. The results show that this method may provide a means for enhancing features such as fog in an automated fashion, as the fog features in the image are subtly distinguished from other low cloud features in the field of view. Clearly, more analysis and validation is required to determine the value of this product.

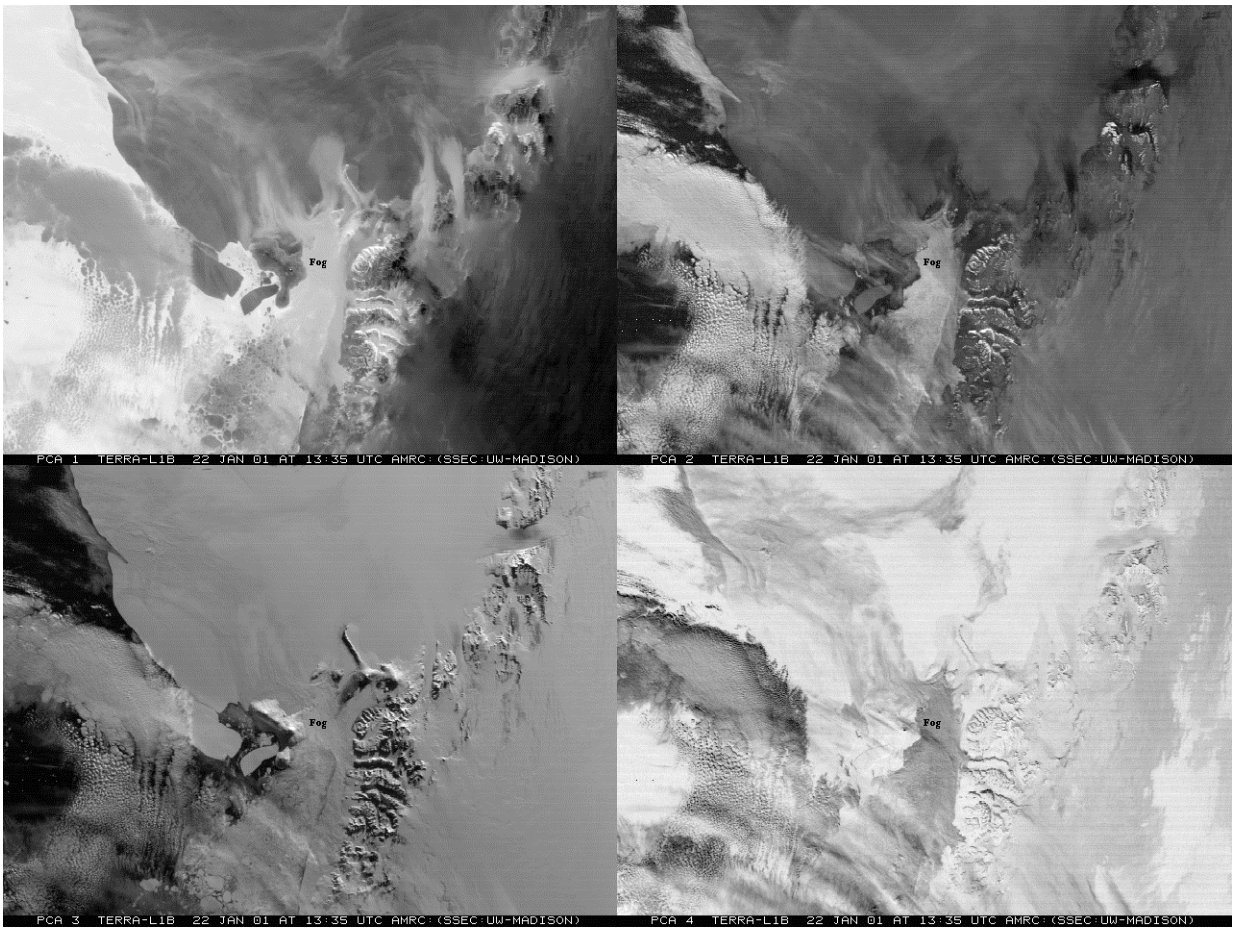

Figure 13. The first four principal component "images" from 8 spectral channels of a sample MODIS image. The top left image is the first principal component, the top right image is the second principal component, the bottom left image is the third principal component, and the bottom right image is the fourth principal component. The fog area is labeled in each image.

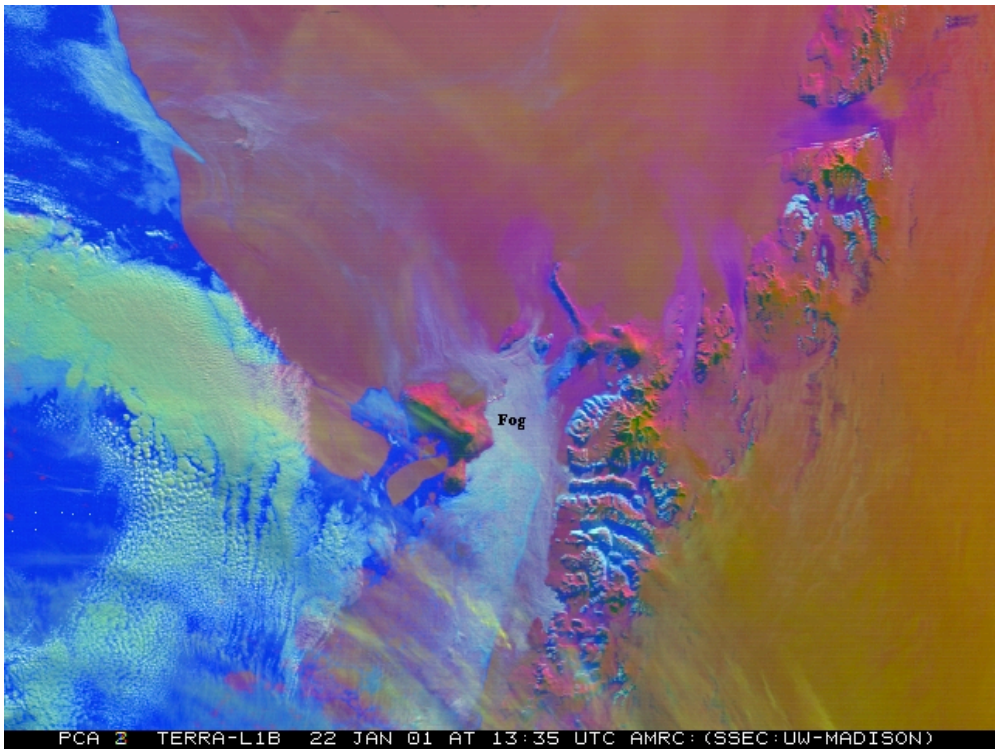

Figure 14. A red-green-blue color combination of the first three principal component images. In this combination fog and other features are enhanced, while others subdued.

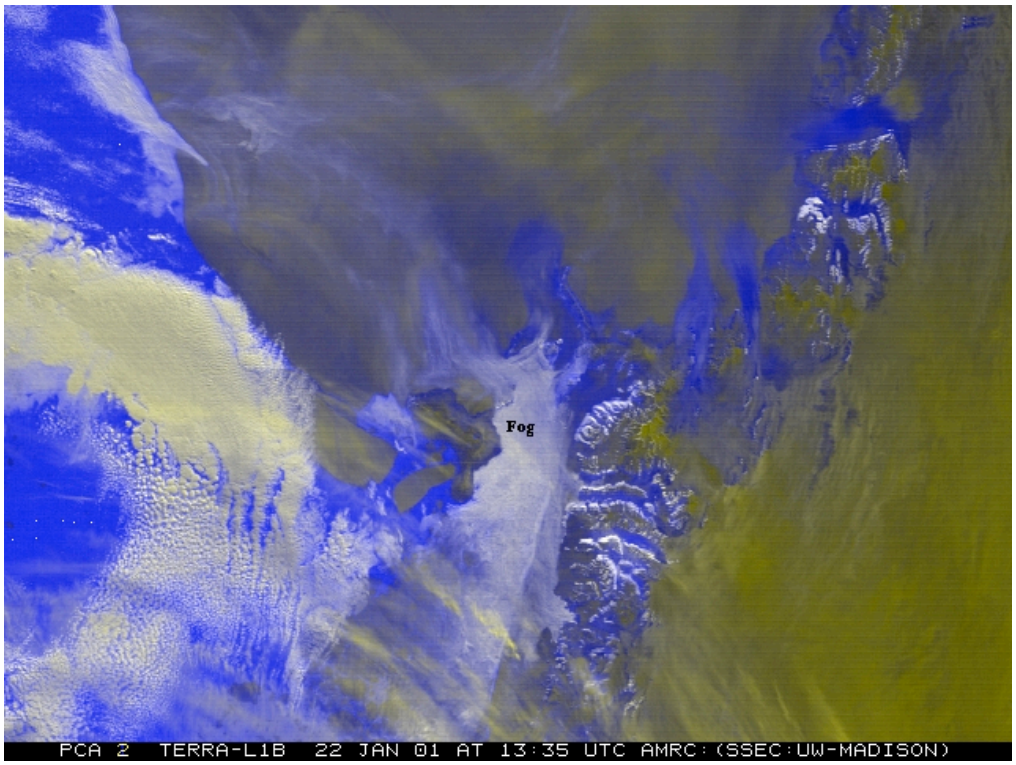

Figure 15. A red-green-blue color combination of the first two principal component images, with weight favoring the second principal component. This combination enhances the fog with moderate clarity.

Spectral Test Methods With Masking

Significant effort has been put into the detection of or "masking" for clouds in satellite imagery (i.e. Ackerman et al., 1998). Hence, one method for detecting fog is to consider detecting clouds/no clouds as a starting point and use the results as a basis for isolating suspected fog areas. Efforts related to this class of method have been under investigation in Europe using both SEVIRI (on the Meteosat Second Generation satellite) and MODIS sensors (Bendix et al., 2003, Bendix et al., 2004, Bendix et al., 2005). Here, based on radiative transfer computations, thresholds in multiple spectral channels are set to distinguish fog from other observations in the satellite imagery (Cermak et al., 2004, Bendix et al., 2004). An example cloud mask product is shown in figure 16, matching the same fog case analyzed in the above sections and figures. Clearly, the standard cloud detection product does not provide correct information over the ice and land areas, labeling them all a clear. However, over the oceanic region, there is skill in depicting clouds probabilities within the field of view. Despite a few errors or uncertainties in this method, the 18 different spectral tests that go into this product are a launching point to filtering out the low cloud and possible fog from the rest of the scene. This method has yet to be applied to the Antarctic, and is under consideration at the University of Wisconsin.

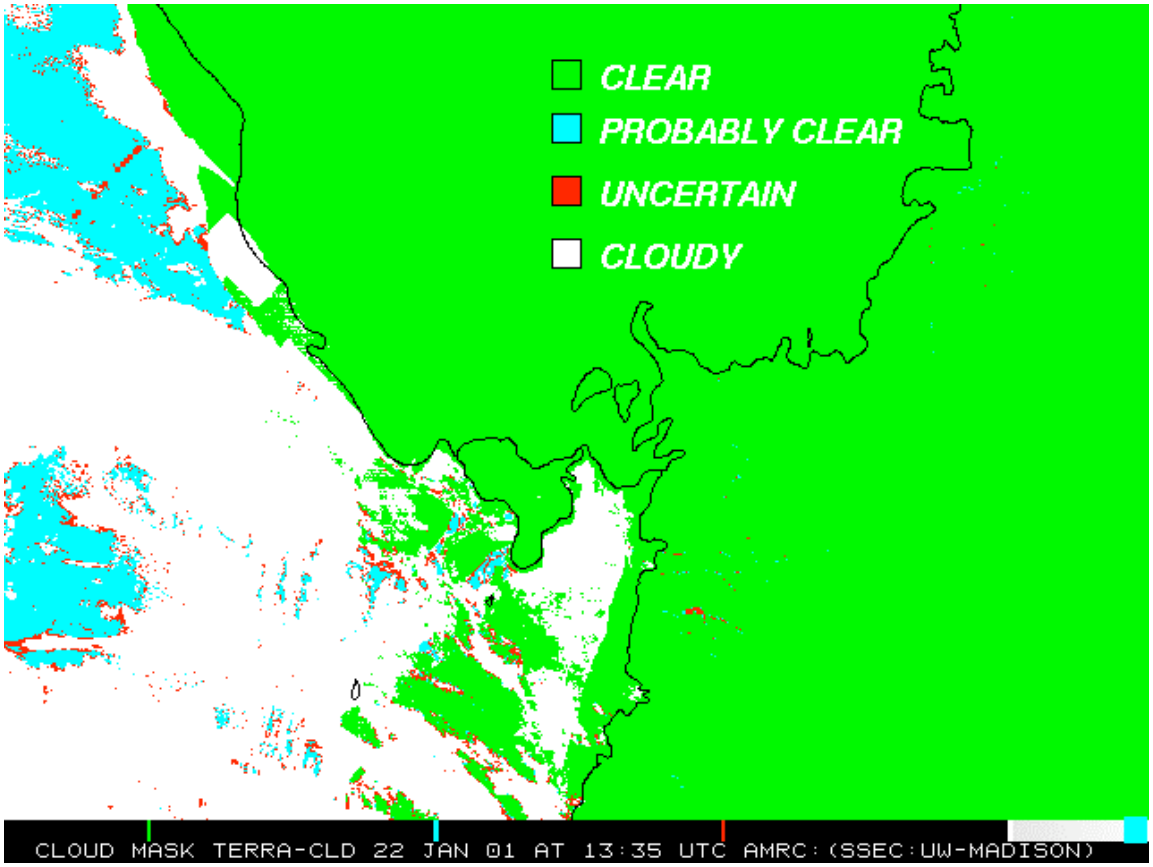

Figure 16. The standard cloud mask from the same fog example case, 22 Jan 2001 at 13:35 UTC. The results show that the standard cloud mask method does not properly classify scenes over the ice/land areas and marks them incorrectly clear.

Case Study: January 16-18, 2004

To demonstrate some of the aspects of fog detection and monitoring, a partial case study is presented here. The fog events on the 16th through 19th of January 2004 provide such an opportunity. It provides a situation that is perhaps more typical of austral summer season fog events – fog mixed with other cloud types and perhaps associated with precipitation occurrences. The case outlined here includes as much as is completed at the time of publication of this report. Additional information is and will be available on the AMRC fog web site as mentioned in Appendix A.

Synoptic Situation

The situation before start of these fog events is perhaps not uncommon for the McMurdo Station area. McMurdo and the Ross Island region is away from major synoptic scale storm systems, and is on the fringes of high pressure and trailing middle latitude frontal system (See Figure 17). Although the surface synoptic flow is weak in the region, generally the direction of the flow is from off the Ross Sea onto the Eastern Ross Ice Shelf, then curving toward the Western Ross Ice Shelf, and then onto the McMurdo Station area.

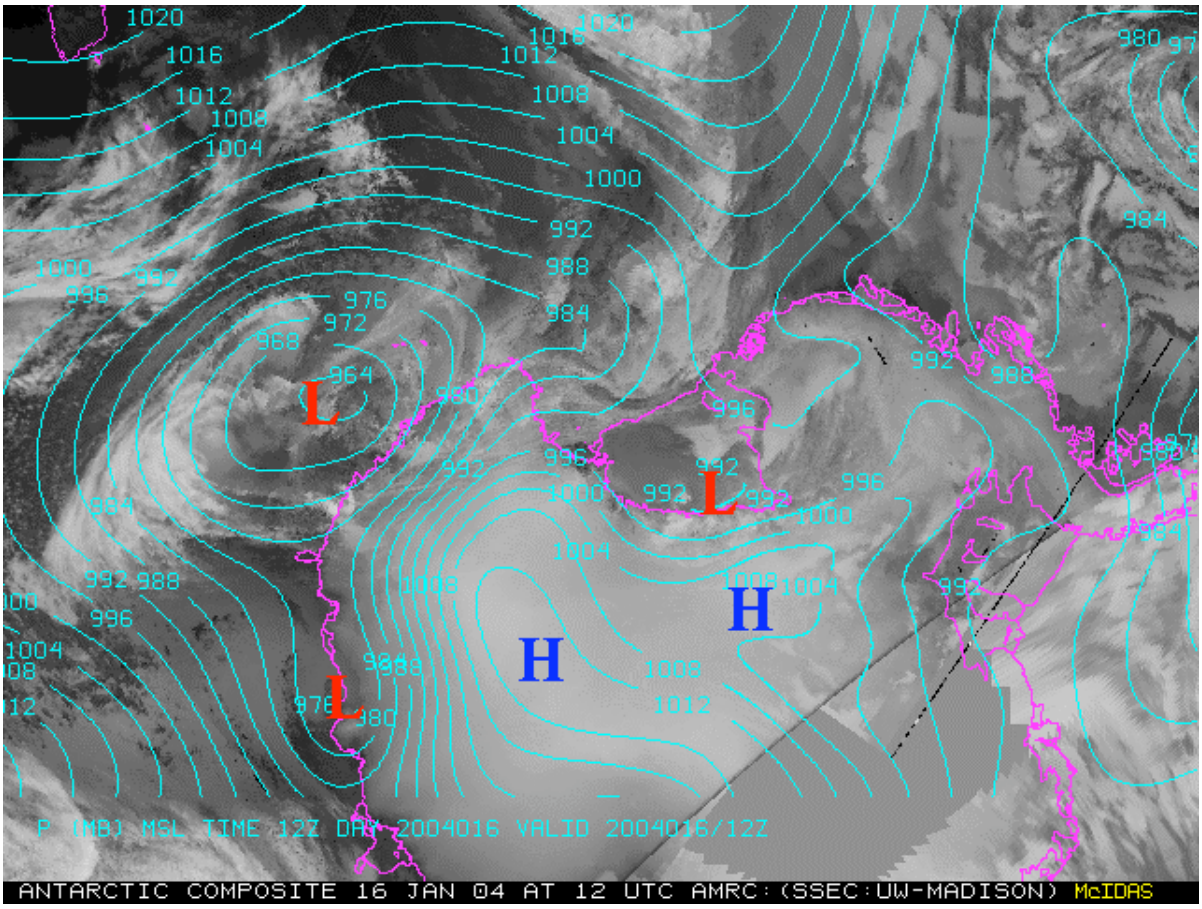

Figure 17. The synoptic situation as of 16 January 2004 at 12 UTC as depicted via the Antarctic composite satellite overlain with the surface isobaric analysis from the Global Forecast System (GFS).

Surface Observations

Reviewing the events from ground based observations reveals that three episodes of fog occurred during this time period, each couched in precipitation events (See Figures 18 through 21). The meteorogram from Williams Field denotes fog occurrences on the 16th at 14 UTC through the 17th at 2 UTC, again at 15 UTC through 23 UTC on the 17th (as reported in the raw observations not shown here), and finally on the 19th at 18 UTC through 21 UTC. Each of these events is followed by or accompanied by precipitation. Pressure and temperature track very well between the stations, capturing the regional situation. Relative humidity values at the AWS sites also closely track the fog events with a slight lag – which takes into account the distances between the stations. As noted in Appendix E, Ferrell AWS site has been historically used as an early warning AWS site for the arrival of fog in the McMurdo area (NSFA, 1990). It is important to note that Ferrell AWS site has been moving with the ice shelf, roughly averaging 0.7 kilometers movement per year, placing Ferrell AWS significantly further North than its original installation location (Weidner, pers. comms., 2005). More recently, weather forecasters employ an empirical technique for forecasting fog as outlined in Appendix D using the UW-Madison and SPAWAR AWS network in the McMurdo Sound basin.

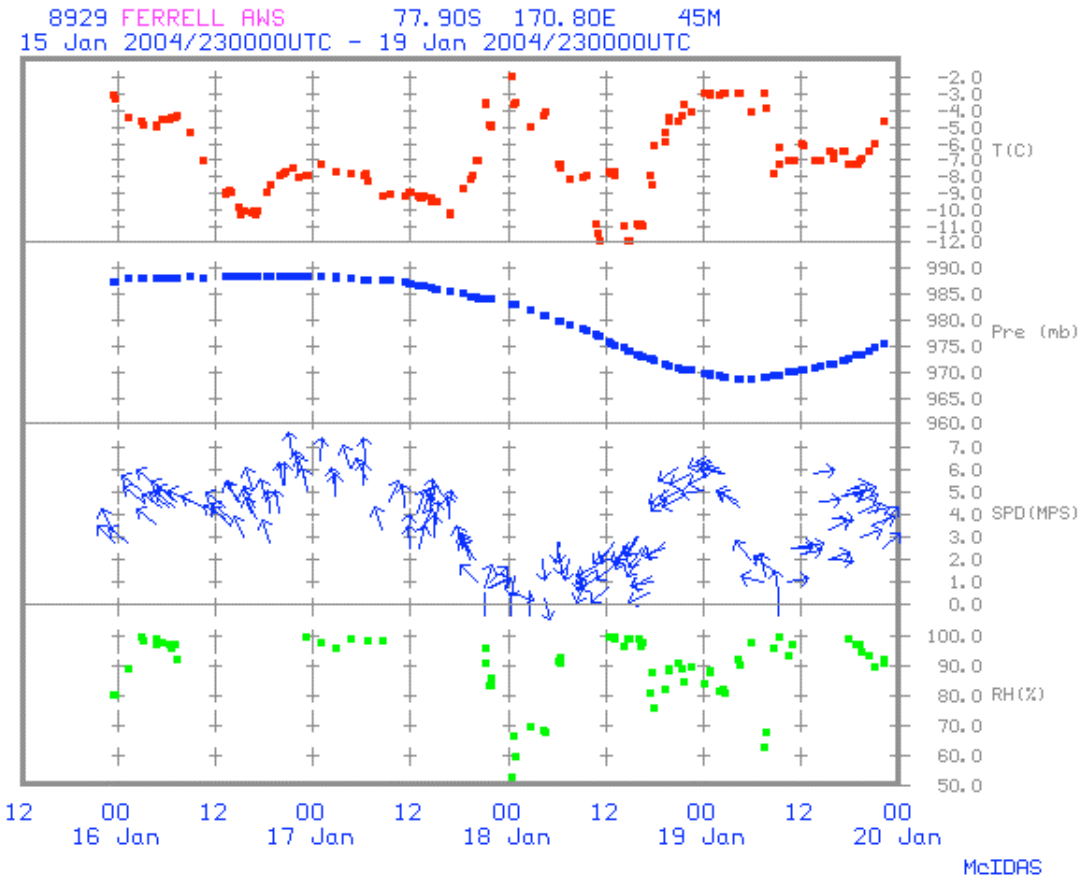

Figure 18. Ferrell AWS meteorogram from 00 UTC 16 Jan through 00 UTC 20 Jan 2004 during the multiple fog events.

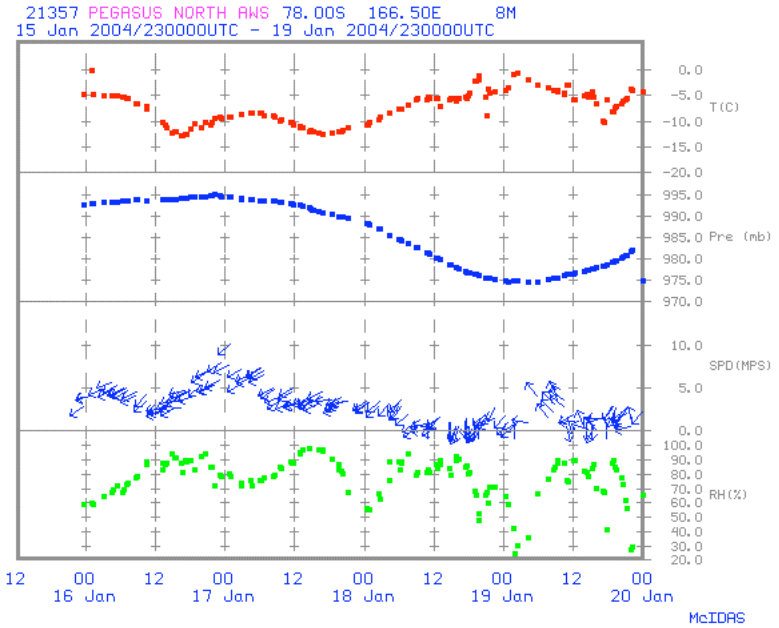

Figure 19. Pegasus North AWS meteorogram from 00 UTC 16 January through 00 UTC 20 January 2004 during the multiple fog events.

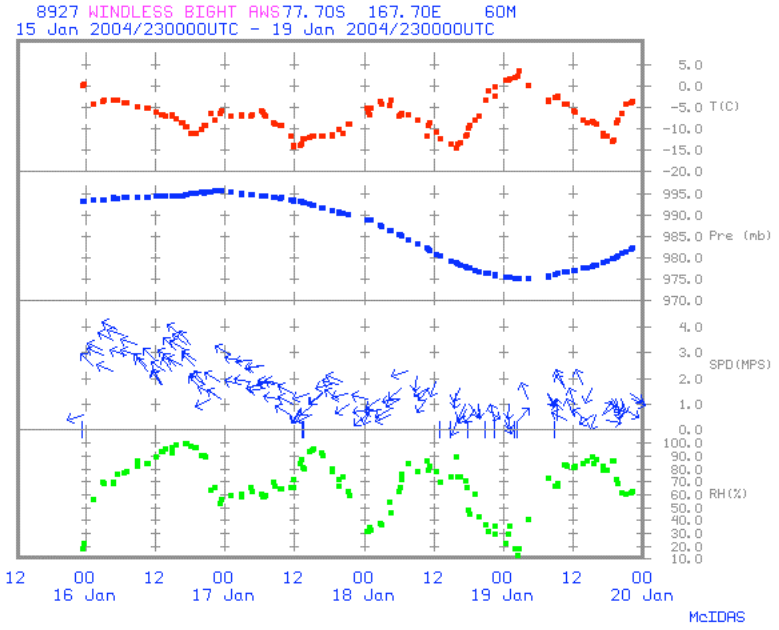

Figure 20. Windless Bight AWS meteorogram from 00 UTC 16 January through 00 UTC 20 January 2004 during the multiple fog events.

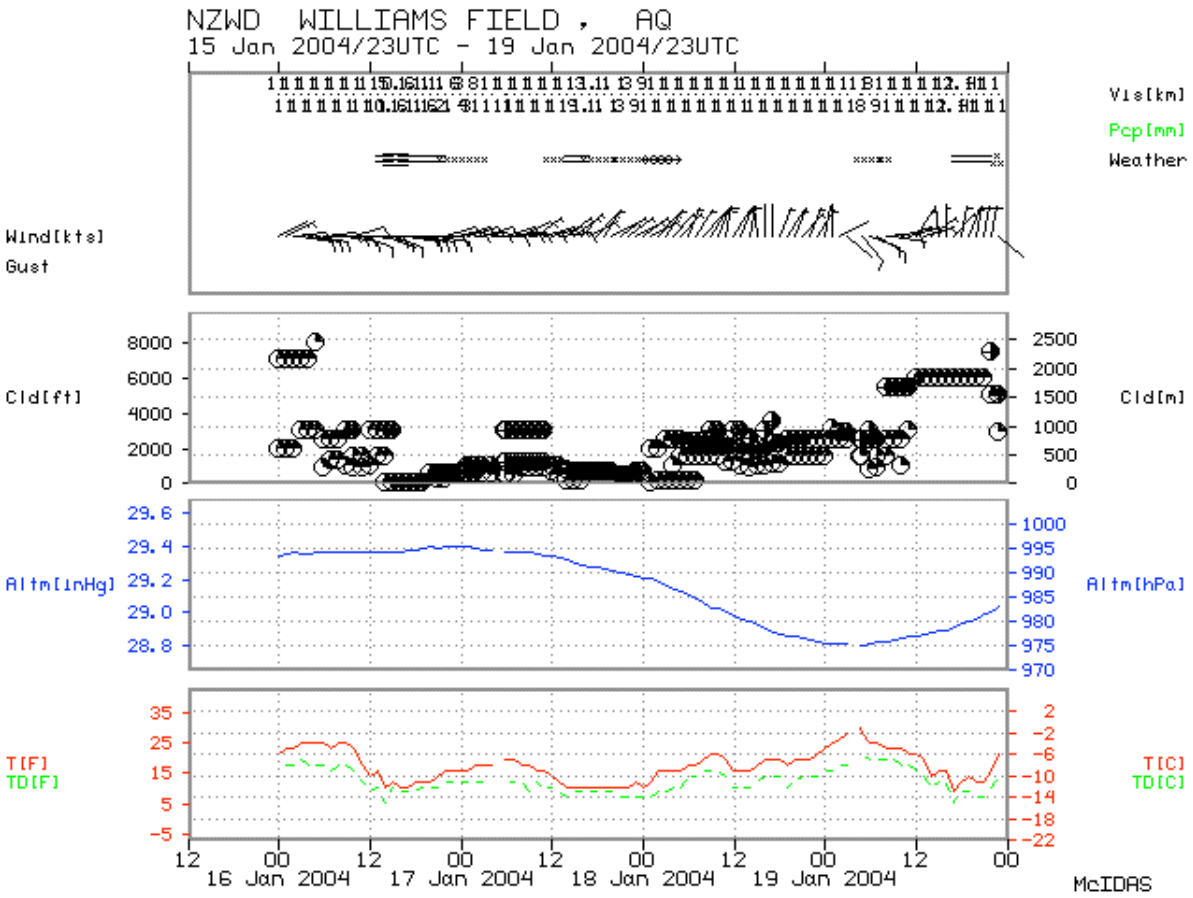

Figure 21. Williams Field METAR meteorogram depicting surface conditions before and during the multiple fog events from 00 UTC 16 January through 00 UTC 20 January 2004. Note that unlike the AWS displays in figures 18 through 20, which have wind vectors, the above METAR observations have wind barbs.

Visible Satellite with Surface Observations

The satellite visible animation during this period, overlain with the surface observations (See sample in figure 22), shows how the low cloud and fog ebb and flow around the region. Clouds seen in the imagery reveal characteristics not uncommon to the region – low clouds, and in some cases such as this one, partially transparent. One of the most powerful uses of the quarter kilometer high resolution imagery is the detail afforded by that improved resolution over the nominal one kilometer found on most polar orbiting satellite imagers. As can be seen in this still image and more vividly in the animation found on the case study web site (See Appendix A for the address), the complex movement of clouds and fog are fairly well depicted at this higher resolution. Critical aspects to exploiting this data requires the remapping of the data into a consistent navigation/projection as well a manual contrast stretch of each image.

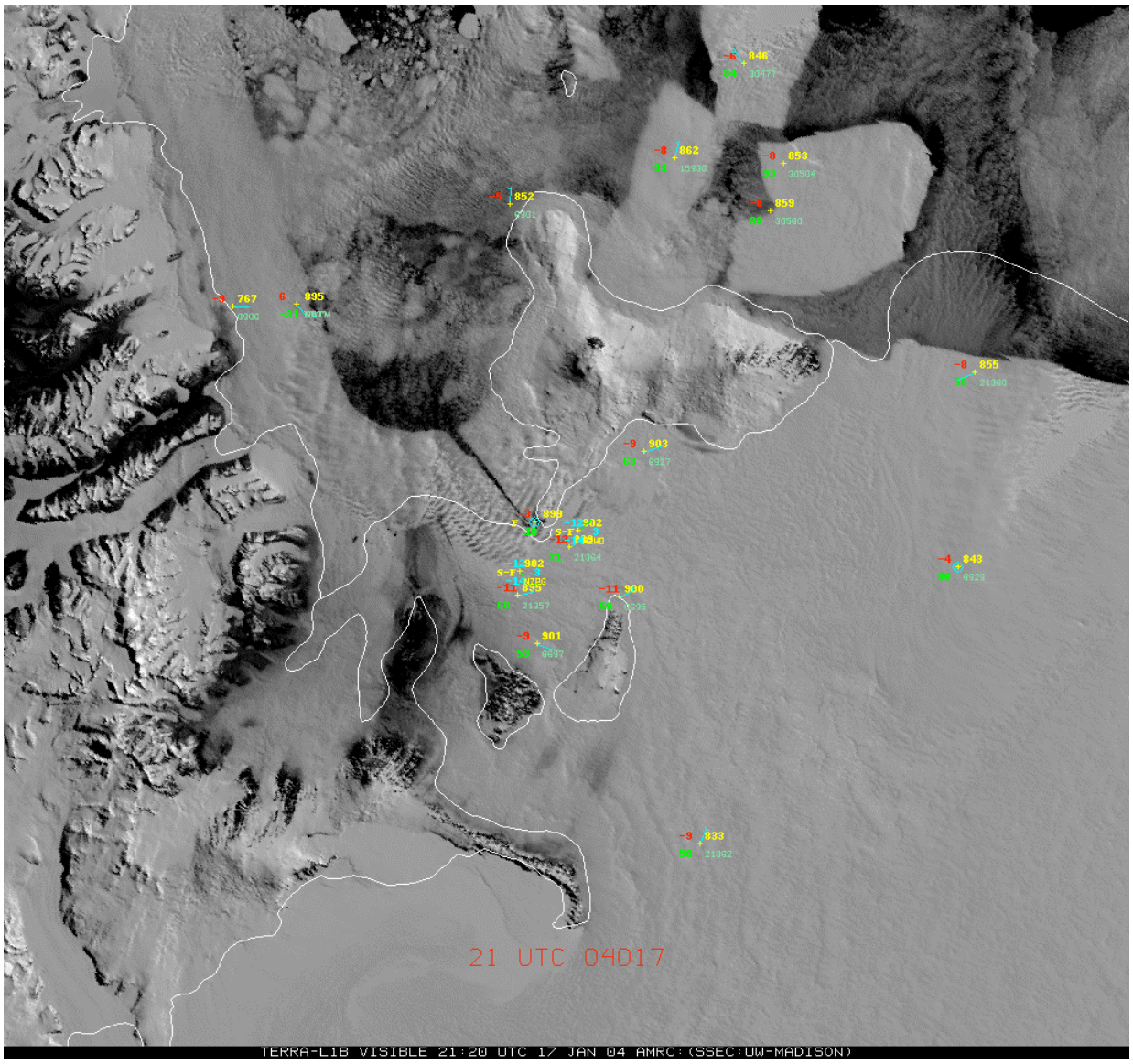

Figure 22. A display of the visible channel MODIS observations from the Terra satellite at 250 meter resolution with AWS, METAR and Ship observations overlain at 21:20 UTC 17 Jan 2004.

Radiosonde Observations

Figures 23 and 24 shows a series of radiosonde observations, plotted in the boundary layer from the raw ascent data from McMurdo Station, Antarctica. The series shows the pre-event and during event conditions of the lowest part of the atmosphere, the moistening and mixed dry layers. These observations are only snapshots of the evolution of the boundary layer through this time period. Note that the data is not corrected for any errors possible due to adjustment, such as in part A of figure 23 and part B and C of figure 24 which have likely unrealistic superadiabatic lapse rates in the very lowest portion of the sounding.

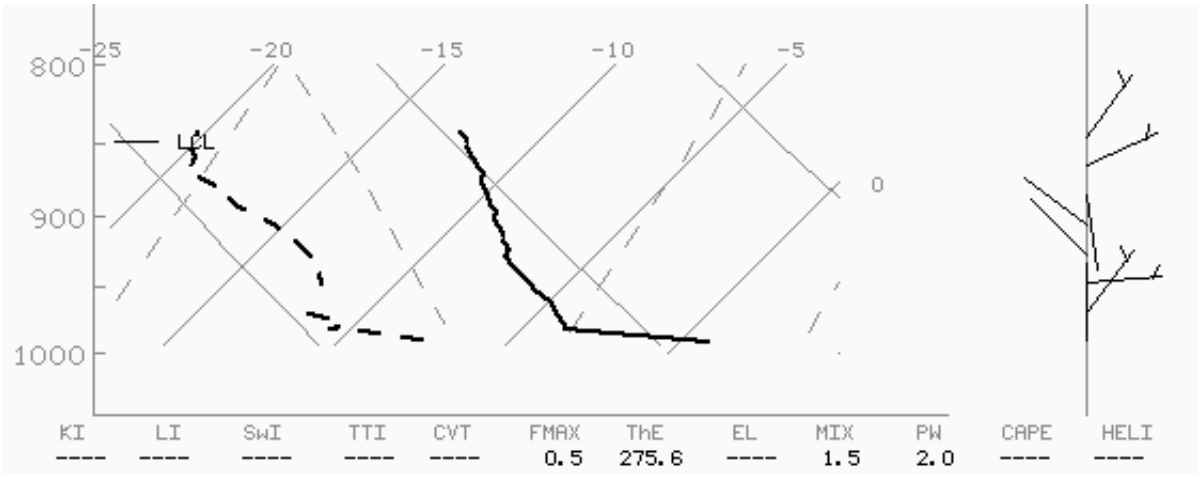

A. 00 UTC 16 JAN 2004

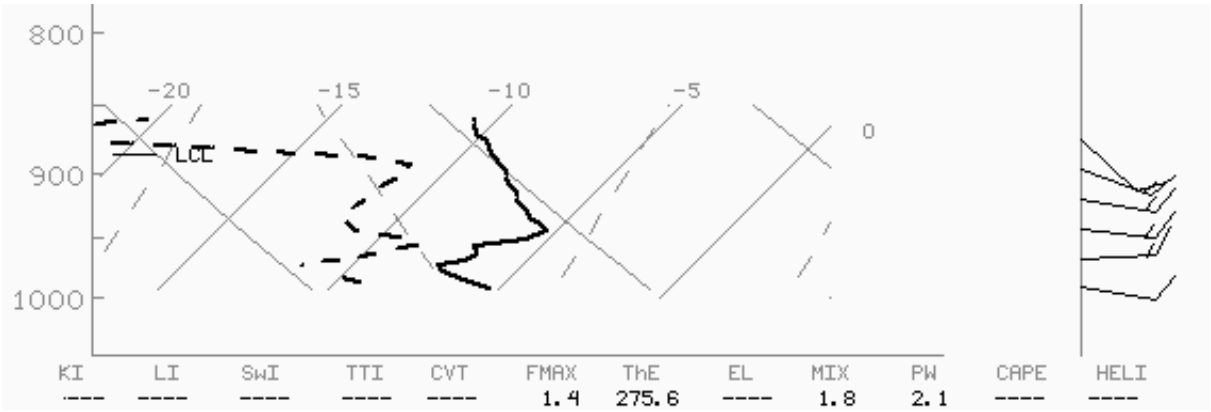

B. 12 UTC 16 JAN 2004

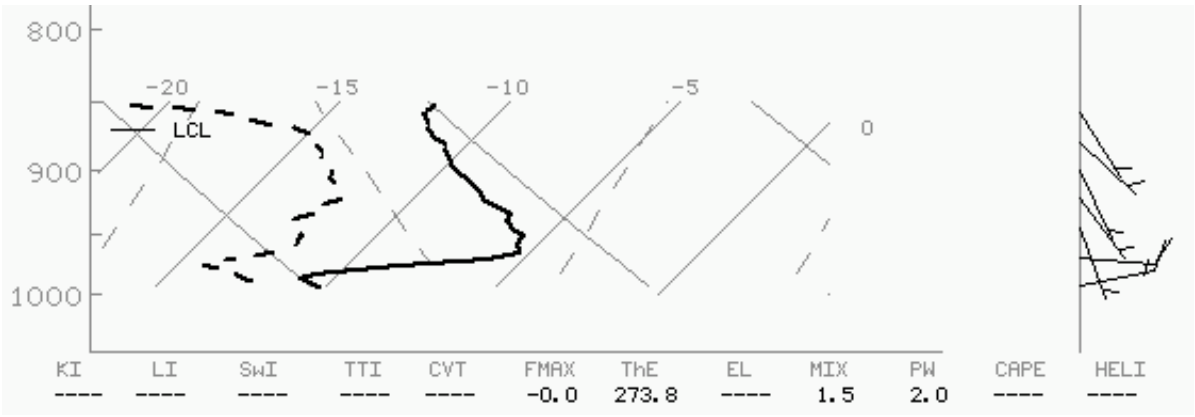

C. 00 UTC 17 JAN 2004

Figure 23. A series of boundary skewT logP diagrams taken from the raw high resolution radiosonde observations from McMurdo Station, Antarctica during the case study period.

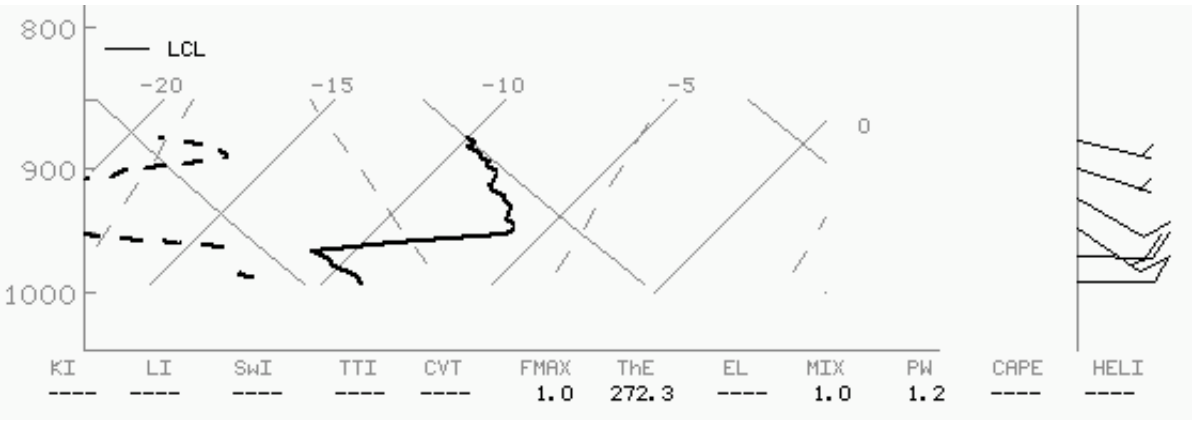

A. 12 UTC 17 JAN 2004

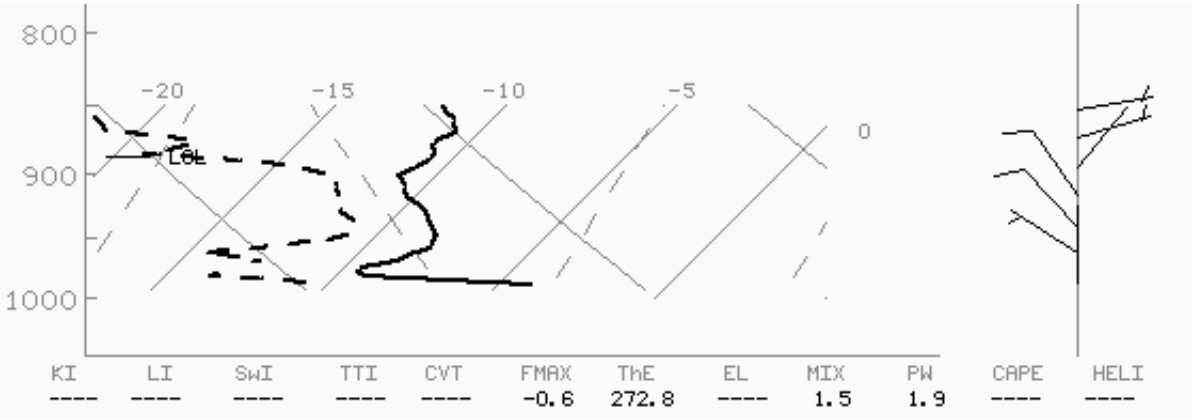

B. 00 UTC 18 JAN 2004

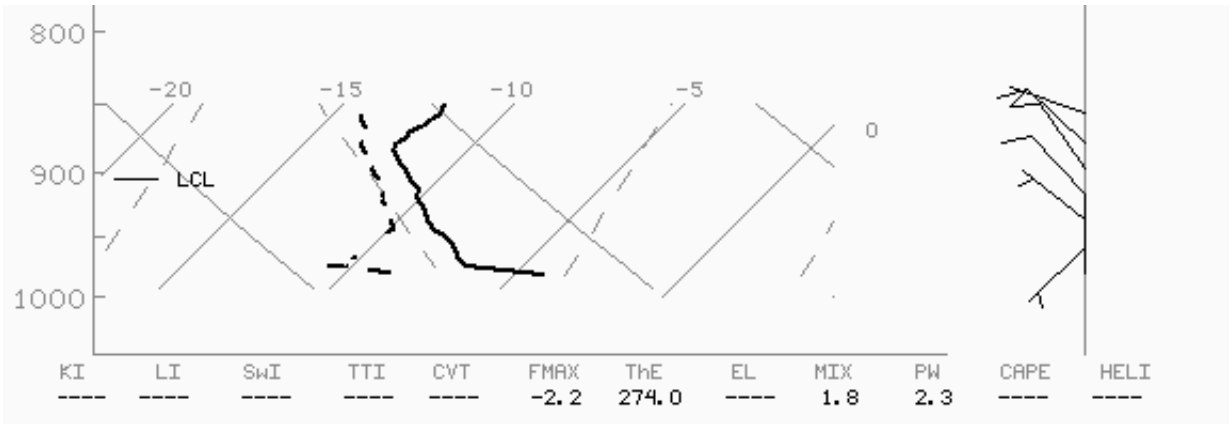

C. 12 UTC 18 JAN 2004

Figure 24. A series of boundary skewT logP diagrams taken from the raw high resolution radiosonde observations from McMurdo Station, Antarctica during the case study period.

Satellite Derived Observations

Many of the satellite-derived products applications introduced in the prior section are shown here during one portion of the fog event at 21:20 UTC 17 January 2004. Figures 25 through 29 are displayed here for comparison of the different depiction methods. In this example, each of the monitoring and detection methods does show a level of skill in detecting the fog and low clouds.

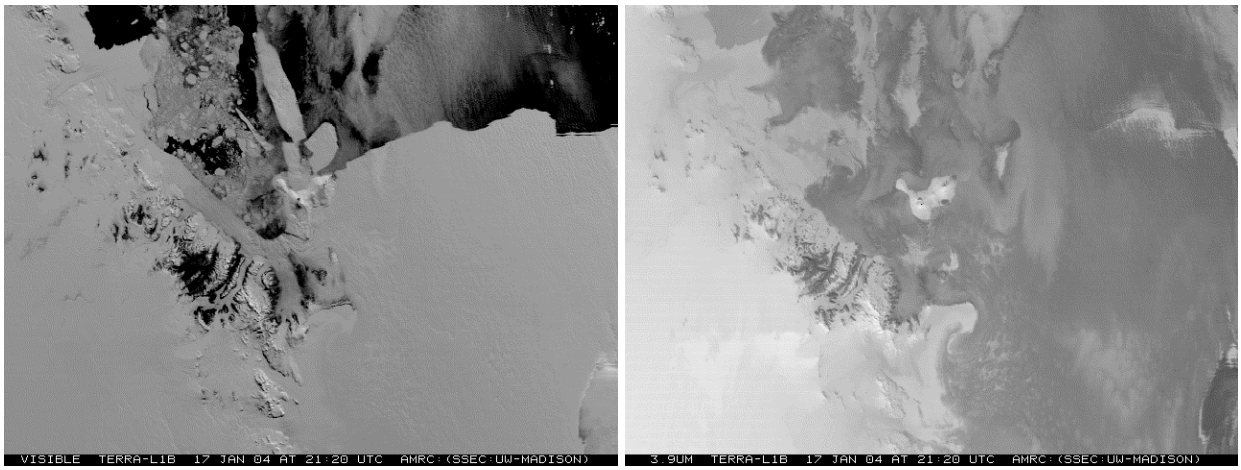

A. B.

Figure 25. ***Single Channel Detection:*** **a. Visible image from the Terra satellite at 21:20 UTC on 17 Jan 2006 and b. the 3.9-micron shortwave infrared image from the same time.**

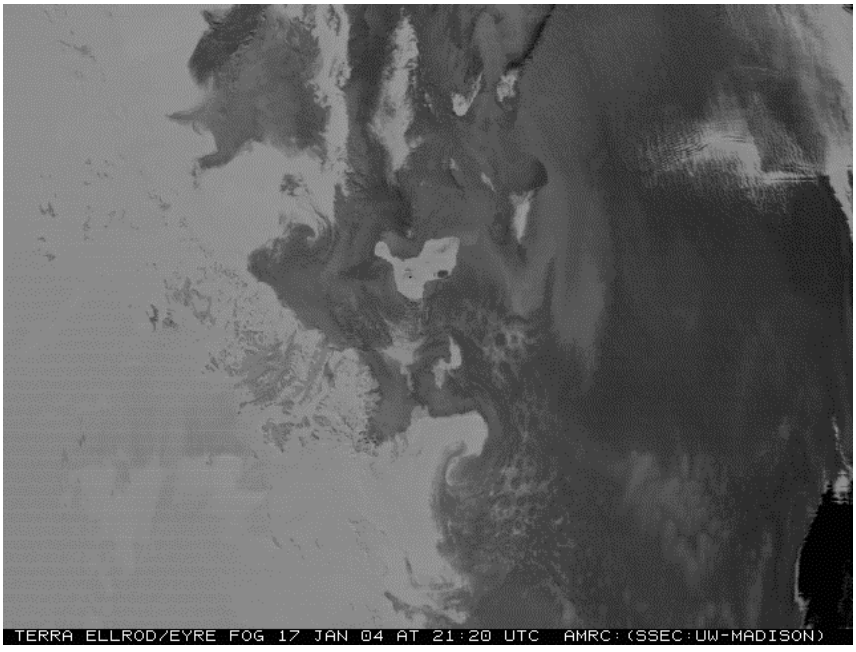

Figure 26. ***Dual Channel Detection*****: The Ellrod-Eyre fog product at 21:20 UTC 17 January 2004. Low cloud and fog are depicted in the darker shades.**

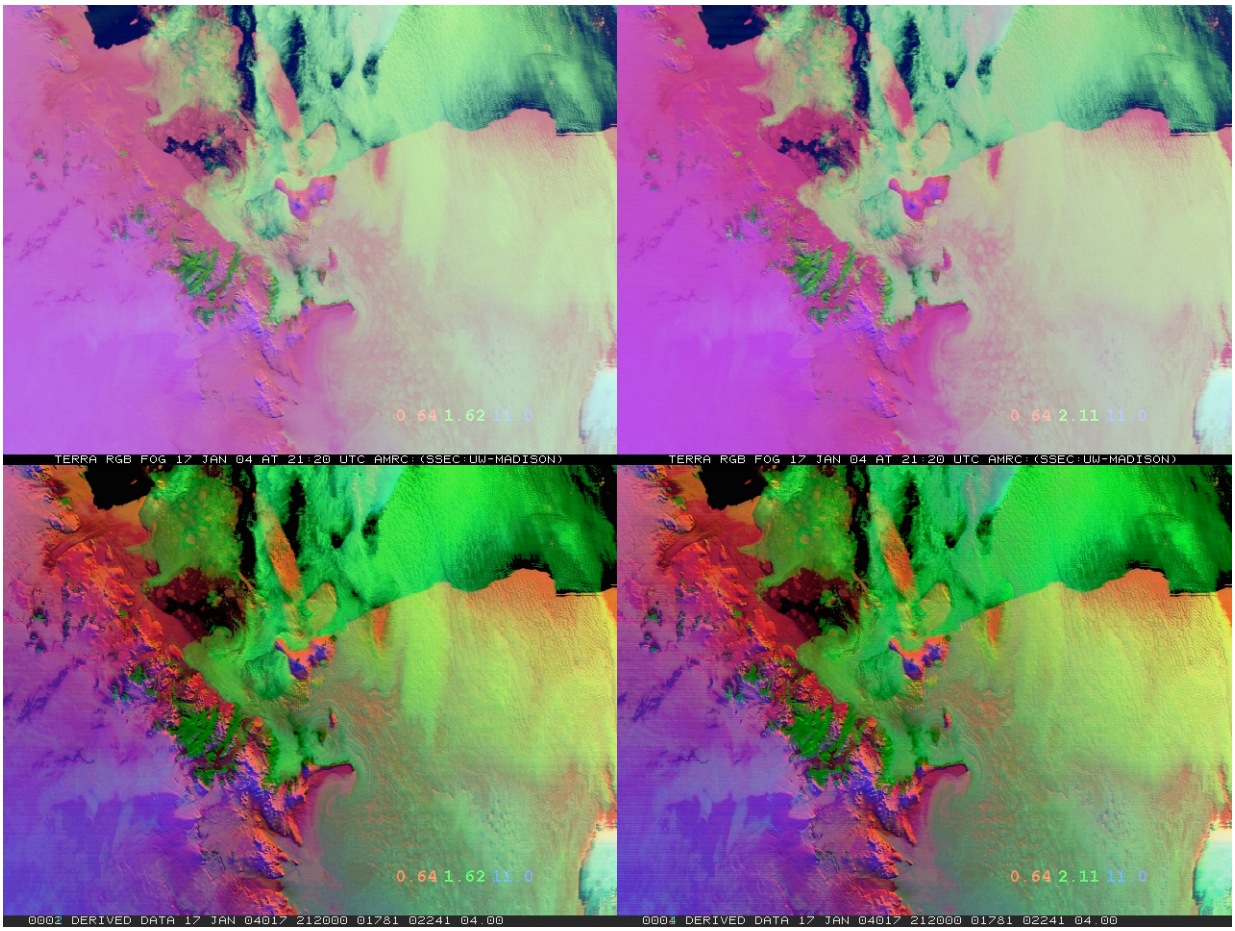

Figure 27. ***Multi-channel Detection:*** **RGB three channel combined displays at 21:20 UTC 17 January 2004. The top images are automatically contrast stretched, while the bottom images are contrast stretched using a histogram styled analysis with 24 bins. The right two images are combinations of 0.64-micron, 1.62-micron, and 11.0-micron wavelengths via red, green, and blue, respectively. The left two images are combinations of 0.64-micron, 2.11-micron, and 11.0-micon wavelengths via red, green, and blue, respectively.**

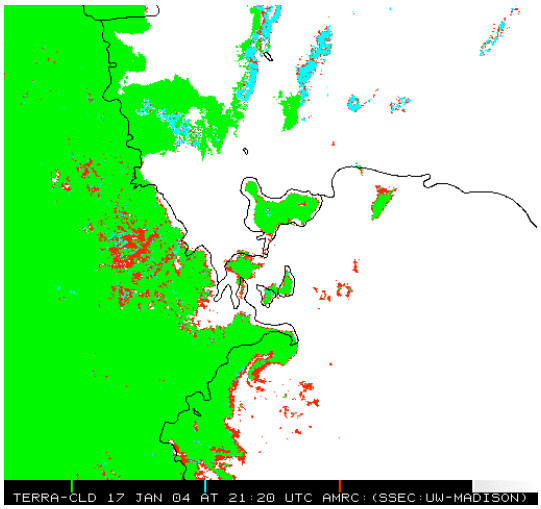

Figure 28. ***Spectral Detection:*** **Standard cloud mask product, similar to Figure 16, from the Terra satellite showing cloud free (green) as well as cloud filled (white) regions in addition to areas of uncertainty (cyan and red).**

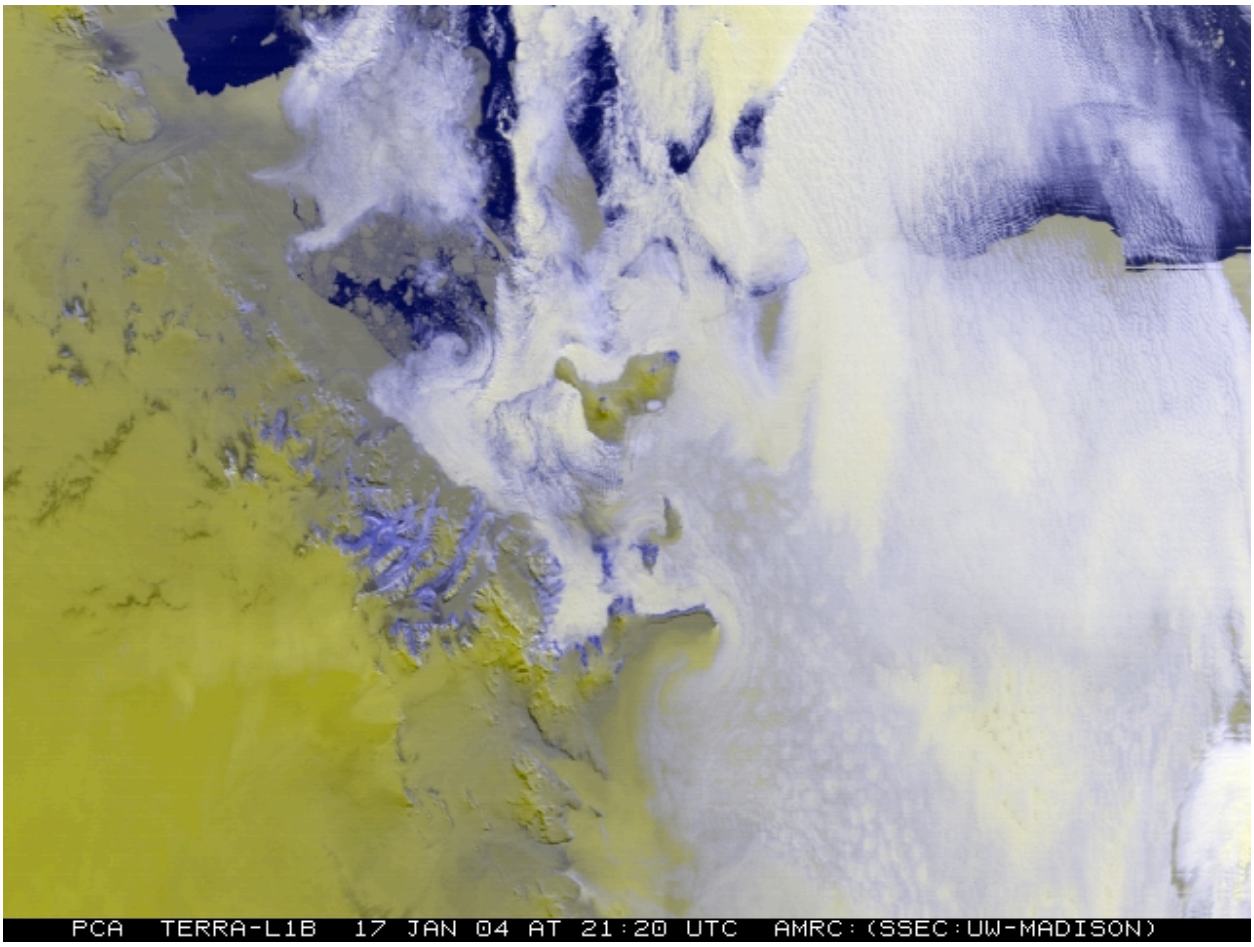

Figure 29. ***PCA Detection:*** **The same display as in Figure 15, however computed for this case study - the weighted first and second principal component analysis imagery combined via red, green and blue with weighting on the second principal component. Note how with moderate clarity the fog and low stratus are depicted, with the thicker low clouds slightly color enhanced.**

Despite each of the methods being able to show some if not many features of the fog and low clouds that are a part of this event, the PCA method may offer a consistent means of automatically enhancing features. As noted, these methods are still under study, and any methods outlined will need verification and validation studies conducted.

Future Satellite Sensor Systems: VIIRS

Description

A full description of the VIIRS sensor system is given in Appendix C of this report. The VIIRS sensor will fly on the NPP and later NPOESS satellite series. With the recent congressional review of the NPOESS program, the NPP satellite will be launched later this decade in 2009, with the NPOESS series to follow in the next with the first satellite launch in 2013.

Carry-Over, New and Missing Applications

Despite the smaller array of spectral channels on the VIIRS sensor, it is expected that any applications of the type described in this document done on the MODIS satellite sensor that share common channels as the VIIRS sensor should be able to be done on the NPP and NPOESS satellite series. Hence most MODIS products for fog can be derived from VIIRS observations. Although no missing applications are likely, new applications of the observations toward detecting fog are not clear at this time.

Summary and Considerations

It is hoped that this report will serve to aid the USAP and other forecasters with the important issue of detecting and monitoring fog with an eye toward improving fog forecasting. Advanced satellite observations give rise to the potential to apply a variety of means to enhance, highlight and isolate fog. Improvements beyond the single and dual channel methods may be found in multi-channel and differential multi-channel color combinations. Improvements via mathematical combinations are likely, along with smart utilization of cloud masking or detection, although these methods are still being researched. Advanced techniques such as principal component analysis also show preliminary promise. Applications to specific cases and fog events will vary, and more analysis and validation is needed.

With the array of possibilities, it is worth considering that several of these products be computed and produced in real-time and made available to forecasters for evaluation. Efforts to compute these products have started at the Antarctic Meteorological Research Center, and more will be undertaken in the next year or two, with a goal of routine generation in real-time and distributed to interested parties (weather forecasters, researchers, etc.). Combined with an observational data set (e.g. surface METAR/AWS, web camera imagery, etc.) and numerical model output (i.e. Antarctic Mesoscale Prediction System), satellite observations such as those discussed in this document provide the basis for fog forecasting. The improved use of these resources likely increases flight safety for the United States Antarctic Program (USAP).

Acknowledgements

The author would like to thank Professor Steve Ackerman of the Department of Atmospheric and Oceanic Sciences and the Cooperative Institute for Meteorological Satellite Studies, Linda Keller of the Department of Atmospheric and Oceanic Sciences, and Art Cayette of SPAWAR System Center Charleston for their advice and comments on this report. This report was funded by SPAWAR Systems Center Charleston (#N65236-06-P-0133).

References

Ackerman, S.A., K.I. Strabala, W.P. Menzel, R.A. Frey, C.C. Moeller, and L.E. Gumley, 1998 Discriminating clear sky from clouds with MODIS. Journal of Geophysical Research, **103**, 32,141-32,157.

Bendix, J., B. Thies, and J. Cermak, 2004: Fog Detection With Terra-MODIS and MSG-SEVIRI. *Proceedings of the 2003 Meteorological Satellite Conference*, Darmstadt, 427-435.

Bendix, J., B. Thies, J. Cermak, and T. Nauss, 2005: Ground fog detection from space based on MODIS daytime data - a feasibility study. *Weath. and Forecasting*, **20**, 989-1005.

Bendix, J, B. Thies, and J. Cermak, 2003: Fog detection with Terra-MODIS and MSG_SEVIRI. *Proceedings 2003 Met. Sat. Users' Conf. Weimar (Germany), 29.9.-3.10.2003, EUMETSAT,* 429-435.

Cermak, J. Thies, B., and Bendix, J., 2004: A new approach to fog detection using SEVIRI and MODIS data. *Proceedings 2004 Met. Sat. Users' Conf. Prague (Czech Rep.), 31.5.-4.6.2004, EUMETSAT,*

Ellrod, G.P., 1991: Nighttime fog detection with bi-spectral GOES-VAS imagery. *Proceedings, Fourth International Conference on Aviation Weather Systems*. May 24-28, 1991. Paris, France. Amer. Meteor. Soc., 71-75.

Ellrod, G.P., 1994: Detection and analysis of fog at night using GOES multispectral infrared imagery. NOAA Technical Report NESDIS 75, U.S. Department of Commerce, Washington, DC. 22 pp.

Ellrod, G.P., 1995: Advances in the detection and analysis of fog at night using GOES multispectral infrared imagery. *Wea. Forecasting*. **10**, 606-619.

Eyre, J.R., J.L. Brownscombe, and R.J. Allam, 1984: Detection of fog at night using Advanced Very High Resolution Radiometer (AVHRR) imagery. *Meteorological Magazine*, **113**, 266-271.

Hunt, G.E., 1973: Radiative properties of terrestrial clouds at visible and infrared thermal window wavelengths. *Q.J.R. Meteorol. Soc.*, **99**, 346-369.

Hutchison, K.D., and A.P. Cracknell, 2006: Visible Infrared Imager Radiometer Suite: A New Operational Cloud Imager. CRC Taylor & Francis Group, Boca Raton, FL. 230 pp.

Lazzara, M.A., 2006: A McMurdo Station Climatology. UW SSEC Publication No.XX.XX.XX (Draft – unpublished at this time). Space Science and Engineering Center, University of Wisconsin-Madison, 28 pp. [Available from the AMRC, University of Wisconsin-Madison, 1225 W. Dayton St., Madison, WI 53706.]

Lee, T.F, F.J. Turk, and K. Richardson, 1997: Stratus and fog products using GOES-8-9 3.9 micron data. *Wea. Forecasting*, **12**, 664-677.

NSFA, 1990: Forecaster's Handbook. Naval Support Force, Antarctica (NSFA). (Unpublished)

Turner, J., Allam, R.J., and Maine, D.R., 1986: A case study of the detection of fog at night using channels 3 and 4 on the Advanced Very High Resolution Radiometer (AVHRR). *Meteorol. Mag*., **115**, 285-290.

Wetzel, M.A., R.D. Borys, and L.E. Xu, 1996: Satellite mircophysical retrievals for land-based fog with validation by balloon profiling, *Journal of Applied Meteorology*, **35**, 810-829.

Appendix A: On-line Companion Resources

As a companion to this report is a web site hosted by the Antarctic Meteorological Research Center at the Space Science and Engineering Center at the University of Wisconsin-Madison. This web site will offer copies of this report, the analysis of the case study presented here, as well as reports and presentations on the PhD thesis research by the author in the near future. In addition, the site will soon contain real-time examples of fog products from the Direct Broadcast X-band System from McMurdo Station, Antarctica. Other products from satellite reception systems at McMurdo Station, or direct from NOAA or NASA may be available in the near future as well. Readers of this report are encouraged to view these companion materials at:

Main AMRC Fog Project Web Page:

http://amrc.ssec.wisc.edu/fog.html

Fog Case Study 17-19 January 2004:

http://amrc.ssec.wisc.edu/~mattl/fog/17-18Jan2004/fogcase_17-18_Jan_2004.html

AMRC Draft McMurdo Climatology Review:

http://amrc.ssec.wisc.edu/~mattl/fog/McMurdo-Climatology.doc

This report:

http://amrc.ssec.wisc.edu/Satellite-Appllications-Report.pdf

Other Satellite Reports:

http://amrc.ssec.wisc.edu/SPAWARSatellite-Report2002.pdf
http://amrc.ssec.wisc.edu/Satellite-Report2004.pdf
http://amrc.ssec.wisc.edu/Satellite-Report2006.pdf
http://amrc.ssec.wisc.edu/Polar-Decadal.pdf

Appendix B: MODIS Technical Specifications

From http://modis.gsfc.nasa.gov/about/specs.html

Spacecraft:
Terra and Aqua satellites

Orbit:
705 km, 10:30 a.m. descending node (Terra) or 1:30 p.m. ascending node (Aqua), sun-synchronous, near-polar, circular

Scan Rate:
20.3 rpm, cross track

Swath Dimensions:
2330 km (cross track) by 10 km (along track at nadir)

Telescope:
17.78 cm diam. off-axis, afocal (collimated), with intermediate field stop

Size:
1.0 x 1.6 x 1.0 m

Weight:
228.7 kg

Power:
162.5 W (single orbit average)

Data Rate:
10.6 Mbps (peak daytime); 6.1 Mbps (orbital average)

Quantization:
12 bits

Spatial Resolution:
250 m (bands 1-2)
500 m (bands 3-7)
1000 m (bands 8-36)

Design Life:
6 years

Primary Use	Band	Bandwidth[1]	Spectral Radiance[2]	Required SNR[3]
Land/Cloud/Aerosols Boundaries	1	620 - 670	21.8	128
	2	841 - 876	24.7	201
Land/Cloud/Aerosols Properties	3	459 - 479	35.3	243
	4	545 - 565	29.0	228
	5	1230 - 1250	5.4	74
	6	1628 - 1652	7.3	275
	7	2105 - 2155	1.0	110
Ocean Color/ Phytoplankton/ Biogeochemistry	8	405 - 420	44.9	880
	9	438 - 448	41.9	838
	10	483 - 493	32.1	802
	11	526 - 536	27.9	754
	12	546 - 556	21.0	750
	13	662 - 672	9.5	910
	14	673 - 683	8.7	1087
	15	743 - 753	10.2	586
	16	862 - 877	6.2	516
Atmospheric Water Vapor	17	890 - 920	10.0	167
	18	931 - 941	3.6	57
	19	915 - 965	15.0	250

[1] Bands 1 to 19 are in nm; Bands 20 to 36 are in μm

[2] Spectral Radiance values are (W/m2 -μm-sr)

[3] SNR = Signal-to-noise ratio

Primary Use	Band	Bandwidth[1]	Spectral Radiance[2]	Required NE[delta]T(K)[4]
Surface/Cloud Temperature	20	3.660 - 3.840	0.45(300K)	0.05
	21	3.929 - 3.989	2.38(335K)	2.00
	22	3.929 - 3.989	0.67(300K)	0.07
	23	4.020 - 4.080	0.79(300K)	0.07
Atmospheric Temperature	24	4.433 - 4.498	0.17(250K)	0.25
	25	4.482 - 4.549	0.59(275K)	0.25
Cirrus Clouds	26	1.360 - 1.390	6.00	150(SNR)[3]
Water Vapor	27	6.535 - 6.895	1.16(240K)	0.25
	28	7.175 - 7.475	2.18(250K)	0.25
Cloud Properties	29	8.400 - 8.700	9.58(300K)	0.05
Ozone	30	9.580 - 9.880	3.69(250K)	0.25
Surface/Cloud Temperature	31	10.780 - 11.280	9.55(300K)	0.05
	32	11.770 - 12.270	8.94(300K)	0.05
Cloud Top Altitude	33	13.185 - 13.485	4.52(260K)	0.25
	34	13.485 - 13.785	3.76(250K)	0.25
	35	13.785 - 14.085	3.11(240K)	0.25
	36	14.085 - 14.385	2.08(220K)	0.35

[1] Bands 1 to 19 are in nm; Bands 20 to 36 are in μm
[2] Spectral Radiance values are (W/m2 -μm-sr)
[3] SNR = Signal-to-noise ratio
[4] NE(delta)T = Noise-equivalent temperature difference

Note: Performance goal is 30-40% better than required

Appendix C: VIIRS Technical Specifications

From resources at http://npoesslib.ipo.noaa.gov/u_listcategory_v3.php?50

Spacecraft:
NPP and NPOESS satellites
Orbit:
833 km, nominal cross times of 13:30, 17:30 21:30
sun-synchronous, polar orbiting
Scan Rate (Period):
1.786 seconds
Swath Dimensions:
+/- 56.063 degrees, 3029 km scan
Telescope:
19.1 cm aperture
114 cm focal length
Size:
65 x 129 x 138 cm
Weight:
160-199 kg
Power:
134 W (177 W Peak)
Data Rate:
10.8 Mbps (peak); 6.7 Mbps (orbital average)
(Using 2:1 Rice compression)
Spatial Resolution:
0.371 km (I channels)
0.742 km (M channels)
Design Life:
7 years (plus 8 years storage)

Table 1. The channel listing information for the VIIRS (*adapted from Hutchison & Cracknell, 2006*)

Band Number	VIIRS Channel Designator	Central Wavelength (um)	Bandwidth (um)
1	DNB	0.7	0.4
2	M1	0.412	0.02
3	M2	0.445	0.018
4	M3	0.488	0.020
5	M4	0.555	0.020
6	I1	0.640	0.080
7	M5	0.672	0.020
8	M6	0.746	0.015
9	I2	0.865	0.039
10	M7	0.865	0.039
11	M8	1.240	0.020
12	M9	1.378	0.015
13	I3	1.610	0.060
14	M10	1.610	0.060
15	M11	2.250	0.050
16	I4	3.740	0.380
17	M12	3.700	0.180
18	M13	4.050	0.155
19	M14	8.550	0.300
20	M15	10.763	1.000
21	I5	11.450	1.900
22	M16	12.013	0.950

DNB = 0.742 km resolution at nadir and at 55.8 degrees
I channels = 0.371 km resolution at nadir and 0.8 km at 55.8 degrees
M channels = 0.742 km resolution at nadir and 1.6 km at 55.8 degrees

Appendix D: SPAWAR Empirical Fog Forecasting Technique

Forecasters from the McMurdo Weather Office/SPAWAR (Cayette, pers. comms. 2005) have developed the following empirical fog forecasting method:

At each of the weather observing locations (airfield, AWS site, etc.) compute the following:

	Example:
1. Take last night minimum temperature (24 hour local data)	-14.9 ^{o}C
2. Take 0 UTC dew point/frost point temperature	-13.0 ^{o}C
3. Take the colder of the two in steps 1 and 2	-14.9 ^{o}C
4. To get fog, this colder of the two temperatures is the target temperature:	-14.9 ^{o}C

5. If the forecast next night's temperature (forecasted by Mac Weather using numerical model output (e.g. AMPS) combined with other methods) is expected to be equal or colder than this target temperature, you have reached the target temperature for fog formation.

6. Additional conditions that must be met:

    a. The relative humidity must 80% or higher at the surface
    b. The temperature and dewpoint temperature spread (dew point depression) must be 4 ^{o}C or less.
    c. Winds are 10 knots (5.1 meters per second) or less.
    d. No clouds are below 7,000 feet (~2134 meters) as a ceiling: overcast or broken (not scattered or few)– and at least with ½ of the sky having coverage.
    e. This method no longer works the day after fog forms; hence use only on first fog formation.

If the above conditions are met, fog is forecasted. An additional impact on the method reported by forecasters is the surface conditions (e.g. fresh snowfall, etc.) and month of the year impacting this procedure's outcome.

Appendix E: NSFA Fog Forecasting Rules for McMurdo Station

The following is reproduced from the 1990 Naval Support Force, Antarctica (NSFA) Forecaster's Handbook (NSFA, 1990 pages III-7 and V-6 through V-8):

Fog

Fog is most common from January to March. Fog will often develop and dissipate or move with no warning. Two synoptic situations have been found that lead to fog at Williams field.

a. *High pressure center just north of ice edge*. This will produce a light northerly flow over the area which will advect in moisture from the open water north of Ross Island. Diurnal cooling then forms fog. Occasionally, a low bank of stratus with bases near 800 feet is advected in from the north and spread out over the ice shelf. After approximately 1-3 hours this stratus lowers to the surface producing dense fog. This fog usually burns off by 1000L. As long as the high continues to advect moisture into the area fog is possible.

b. *Low pressure system over the ice shelf*. Fog normally occurs around the periphery of a low over the Ross Sea or Ice Shelf. This fog will continue during the coolest part of the evening until the low dissipates or moves off.

The McMurdo forecasting rule section (below) discusses most of the empirical rules on forecasting fog. One of the most accurate rule is based on the Ferrell AWS station. If the wind at Ferrell shifts to the southeast (100-170 degrees), fog will develop at Williams Field within 3-8 hours, reducing visibility to ½ mile or less. This is accurate if the wind is greater than 3 knots, the shift occurs in the mid to late afternoon or evening, and the sky is clear to partly clouds allowing radiation cooling. This southeast wind is part of a circulation pattern that advects moisture onto the ice shelf.

General

1. Radiation fog alone is rare, but diurnal cooling and heating are important
2. Advection fog
    a. Will often be found to the west and southwest of anticyclone centers in the return flow.
    b. Occurs around the periphery of a low over the Ross Sea. Fog will penetrate the southern Ross Sea/Ice Shelf and affect McMurdo, arriving at Williams Field before it can be seen from McMurdo.
    c. Most frequent over Ross Sea during periods of meridonal flow.
    d. Usually shallow 50 to 500 feet thick
    e. Max frequency Dec and Jan (See F02).
3. Ice Fog

a. General
    i. Cold temperatures.
    ii. Low level inversion concentrates moisture in a shallow layer.
    iii. Camp fog may contribute (occurs below -30 ^{o}C)
b. Considerations
    i. Temp is critical - -25 ^{o}C to -35 ^{o}C at McMurdo.
    ii. With McMurdo's average wind, ice fog will be shallow and diffuse.
    iii. Calm winds – Ice fog will become thicker.
    iv. Aircraft can produce ice fog at temperatures of approximately -30 ^{o}C and lower

4. Sea Smoke (or Steam Fog)
    a. General
        i. Developed by cold dry air flowing over open water.
        ii. Form by intense evaporation from the sea surface
    b. Considerations
        i. Usually shallow – can cause a low deck of stratus north of Hut Point
        ii. Does not hinder McMurdo operations.
        iii. Can't occur until there is extensive open water close to McMurdo. Extends seaward 5-8 nm.
        iv. Most common in February and March.
        v. Favorable synoptic situation: Outbreak of continental Antarctic air on a southerly or westerly wind.

Rules

F01: Fog followed by snow: Frequently during early stages of moderate to heavy snow, fog will occur with the snow rapidly reducing visibility below IFR minimums. Usually the wind picks up about 1-3 hours later and blowing snow commences.

F02: Rules for summer advection fog arrive from the south(east) low on the ice shelf.

a. Often preceded by strong surface inversion with Fata Morgana
b. Will persist as long as the surface inversion and easterly flow are maintained.
c. Diurnal variations: will lift to stratus during day with maximum sun angle and return to surface at night or minimum sun angle.
d. Light wind (5-10 knots) may result in WOXOF for 4-6 hours or more.
e. Moderate wind (15-20 knots) will cause rapid fluctuations in ceiling and visibility from W0X0F to W7X1F. Study low level winds carefully.
f. Will persist as long as the low advects fog onto the ice shelf.

F03: Advection fog arriving from the north.

a. Usually occurs under a weak ridge or high located to the east or north of McMurdo.
b. Light northerly winds will advect fog to McMurdo or

c. 24 hours of northerly flow will advect sufficient moisture to McMurdo to product saturation for fog.
d. Radiational cooling may trigger fog.
e. Cooling from surface to 1000 feet produced by drainage wind will lower the temperature in nearly saturated air causing rapid formation of thick fog, bringing below IFR minimum conditions.
f. Scattered to broken stratus near 800 ft. during the afternoon will thicken and gradually lower as sun angle decreases; can produce W0X0F for 4-6 hours or until warming the next day. This low deck can be seen advecting in from the north. It will slowly settle to the surface.
g. Can be very moist and may deposit spectacular rime: significant rime deposition can occur from fog with moist northerly flow. The air is usually moist producing extensive deposits. This has been known to ground helos due ice build up on rotors when left outside.

F04: If the wind at Ferrell AWS shifts to the southeast in the afternoon to evening and is 3 knots or stronger, fog is very likely in 3-8 hours at Williams Field.

- Ross Sea Low considerable distance from McMurdo – local fog patches (summer months) occur over the ice.
- Ridging into the Ross Sea poleward ridge or ridging from a middle latitude high – may produce a northerly flow and advection fog over Ross Ice Shelf and at McMurdo.

Appendix F: SPAWAR Forecast Handbook Excerpt on Fog

The following excerpt on fog is from the 2002 SPAWAR forecast handbook used by the current government/contract forecasters at McMurdo Station:

Fog: Fog occurrence presents the major forecasting challenge in the McMurdo area. Rapid fog formation and/or advection into McMurdo are the norm in all summer season fog occurrences. It is the primary obstruction to visibility during the summer and increases in frequency of occurrence as increasing air temperatures melt the sea ice in the Ross Sea. Heat fluxes and turbulent mixing promote evaporation over the open water producing saturated air within the boundary layer. A synoptic pattern promoting moisture advection and a decrease in the average temperature should raise caution when developing the forecast. There are four types of fog prevalent in the area; station fog, radiation fog, advection fog, and inversion fog.

Station Fog: During the winter months under extreme cold conditions, station fog (camp fog) is formed when an increase in humidity is combined with exhaust from combustion engines. The occurrence of camp fog is limited to the very beginning of the summer season under the restrictions of a cold outbreak, and may occur when temperatures are below -30 ^{o}C. The considerations for forecasting camp fog are:

* Temperature -13 ^{o}F to -31 ^{o}F/ -25 ^{o}C to -35 ^{o}C,
* Calm winds allow thicker camp fog, and
* Internal combustion engines running.

Radiation Fog: A short-range forecasting tool has been developed for the consideration of radiation fog (early morning fog). On all observed occasions, early morning fog occurred with similar trends in temperature, dew/frost point depression, time of day, and cloud cover preceding the onset of fog. From these events the following empirical rule was developed:

* Target Temperature -- the temperature required for the condensation process to begin. This temperature is equal to the frost/dew point temperature at 00Z from the previous day and must be colder than the minimum temperature the previous night. If the previous night's low is colder, that min temp defaults to the new target temperature. This temperature must be reached or expected during the morning hours.
* Cloud Cover -- clouds are improving, expected to improve, or are steady with no ceilings below 7,000ft at the time of reaching the target temperature.
* Frost/dew point depression is maintained at a 6 °C spread or less from 1100Z.
* Relative humidity values of ~80 percent indicated from the Coastal Environmental Stations (CES) AWS sites on the Ice Shelf.

When all three of these criteria have been met, fog can be forecast for the early to mid-morning period. Also, the degree to which they exceed the listed minimum temp can be directly correlated to the intensity and duration of fog expected. The most frequent time frame for radiation fog formation is from 1200Z to 2000Z.

Advection Fog: The most prevalent type of fog is advection fog. Climatologically, it begins in late December, peaking in March. Several conditions may exist which would advect moisture into the McMurdo area. The key to the formation of fog is producing a proper wind flow, a cold surface forcing condensation, and an inversion layer over the moisture source, which traps the moisture so it is not allowed to be lifted and dispersed freely.

The Ross Ice Shelf provides the cold surface and inversions normally set up within a few hundred feet, however, the topographically induced predominant northeast wind flow created by a southerly wind does not promote advection from a moisture source region. Therefore, one of three wind situations must exist to advect moisture over the runway:

1) A direct continuous northerly wind. Normally set up by a small high extending across the Ross Sea and Ice Shelf. Noticed when one or two lows were moving away from Ross Island.

2) Fog or low stratus clouds already existing over the Ice Shelf just east of White Island and a southeast flow on the Ice Shelf pushing the fog into Ross Island. Normally this situation occurs during the final stage of a decaying low just north of McMurdo.

3) North to northeast winds off Cape Crozier and an easterly flow over McMurdo. This could be from an advancing small low-pressure system, an anti-cyclone over the ice shelf, or a combination of the two.

Note: All of these situations must be accompanied by the appropriate temperature requirements to promote condensation, and a trapping layer must extend from the ice shelf over the open water source region.

Circumstances will exist on occasion where a light northerly flow will set up, but the inversion will not extend over the open water. As the saturated air moves southward, it is lifted over the inversion and condensation normally will produce a low cloud layer.

Nearly all fog occurrences are accompanied by easterly winds of 8 knots and falling pressure. This situation will normally lead the forecaster to believe that fog would not be a factor. A documented study on fog occurrence around the perimeter of a blocking ridge, with winds moving from the sea onto the ice with wind >10kts will cause high humidity fluxes. Surprisingly, 80% of the time fog formed under these conditions. With <10 knots, the cause and effect of fog formation was not as evident or as frequent. The cooling effect at slower wind speeds is minimized due to "slow movement of air parcels over the temperature gradient." (Fett, Naval Tactical Applications Guide, page 1B-2)

Stratus cloud formation with on ice flow becomes more frequent with winds much greater than 10 knots. This is caused by high humidity fluxes, an increase in the depth of the mixed layer, and a concentration of moisture below the turbulence-induced inversion. As observed on 25-26 November 1997, the fog became thicker with an increase in wind speed, and visibility increased when the winds finally dropped below 5 knots. With minimal diurnal effects, it is noted that fog can occur almost any time of the day. The most frequent time frame for fog formation is from

1200Z to 2000Z.

Documented are two synoptic situations that produced fog over the McMurdo area. The first is a late season situation, with the abundance of open water around Ross Island. During the passage of a low within the near proximity of Ross Island, the wind flow around the low rapidly advects moisture into the Windless Bight. Fog moves over the runway and may be shrouded by cloud cover. The fog under these conditions is dense enough to drop the runway below minimums. The situation will rapidly change as the wind pattern shifts and the low moves onto the ice shelf. Fog will roll out as quickly as it moves in, normally lasting 1 to 3 hours. For this situation, ensure the following exist:

* Availability of open water near Cape Crozier.
* A low-pressure system moving from the north, projected to pass between Ross Island and 180 degrees longitude.
* Wind pattern around the low that would extend into McMurdo as the low passes.

To provide the most accurate forecast for this situation, look for a low that would produce a tight flow around Ross Island as it passes. The trajectory of the winds must not force a "piling up of moisture" into the Trans-Antarctic's, but allow a free flowing motion around the Island. This low should be located in the eastern Ross Sea (just north of Ross Island), and have a supporting upper level flow that would direct it south onto the ice shelf. Ensure the 700hpa to 400hpa wind patterns support this motion. Calculate the time the winds will push the moisture into the windless bight and continue the motion of the low to calculate the backside when the wind flow will take the fog away.

The second situation is the decaying of low-pressure systems or movement of lows away from McMurdo. Large low-pressure systems that move near Ross Island and become decaying waves will advect moisture onto the ice shelf that becomes fog or low stratus clouds. The low-level winds will tend to disfavor fog advection into the McMurdo area, with Minna Bluff acting as a barrier to the south for layers under 3,000ft. As the low-pressure's circulation breaks down, the fog is allowed to move north in the general flow and spread under the absence of a tight pressure gradient. The natural divergent flow in the Windless Bight promotes a low-level subsidence inversion. On several occasions, an anticyclonic motion can be depicted in stratus clouds over the central ice shelf as the low retrogrades northward and the glacier winds begin. As the flow to the east of McMurdo changes to the southeast, moisture is advected into the Windless Bight promoting fog formation.

The ideal situation for advection fog over McMurdo is the product of a high-pressure center just north of the ice edge. This situation will produce a light northerly flow over the area advecting moisture from the open water north of Ross Island. A northerly flow for 24 hours will advect sufficient moisture into McMurdo to produce saturation. Cooling is then required to form fog. In this situation, heating is frequently advected with the moisture prohibiting fog to form. Occasionally, a low bank of stratus with bases less than 1,000ft is advected in from the north and spreads out over the ice shelf. After approximately 1 to 3 hours, the stratus lowers to the surface producing dense fog. This fog usually burns off by 1000L. As long as the high center persists, fog is possible.

Inversion Fog: This is the most rare situation with three documented occurrences over the past five years. This situation may promote station (camp) fog formation in the colder months, but lack of winter activity during its synoptically evolved situation has not allowed proper documentation and verification to take place. The situation is promoted by a large depression moving slowly or stagnated near Cape Adare. A well-defined occlusion will extend from Victoria Land over Terra Nova Bay and across the Ross Sea. A thermal tongue will develop on the 850 to 700 hPa levels extending south into the McMurdo Sound. Sounding profiles at McMurdo and temperatures from Odell Glacier AWS will reflect this temperature increase. Mesoscale models of AFWA and NCAR will properly depict the thermal signature 24+ hours in advance. At 4+ hours, the area will be cloud free but high levels of moisture (80 to 99%) will be detected on the sounding between 200 to 1,500 feet. The moisture settles with rapid fog formation and expansion over the entire region. In December 2000 this situation developed with fog forming and visibility going from unrestricted to less than ½ mile within a one-hour period. The fog extended over the entire McMurdo Sound and Windless Bight.

Inversion fog from this situation may fluctuate in the winter months with lack of hygroscopic nuclei, as occurred in August 1998, or will show signs of dispersion with daily heating as in December 2000. In either case the fog reforms with similar intensity until the thermal pattern of the 850 to 700 hPa levels indicate removal of the warm air advection.